

# BÆRENDE KONSTRUKTIONER

DANMARKS TEKNISKE HØJSKOLE



STRUCTURAL RESEARCH LABORATORY  
TECHNICAL UNIVERSITY OF DENMARK

Finn Bach, M. P. Nielsen and M. W. Bræstrup

SHEAR TESTS ON REINFORCED CONCRETE T-BEAMS

SERIES V, U, X, B and S

RAPPORT NR. R 120 1980

SHEAR TESTS ON REINFORCED CONCRETE T-BEAMS  
SERIES V, U, X, B and S

by

Finn Bach, lic.techn.

M.P.Nielsen, dr.techn.

M.W.Bræstrup, lic.techn.

Structural Research Laboratory  
Technical University of Denmark



## SUMMARY

The paper reports on 40 static tests and 7 fatigue tests on simply supported T-beams subjected to symmetrical two-point loading. The webs were reinforced with stirrups, generally vertical stirrups.

The purpose of the static tests was, besides to confirm the results of the previous test series reported in [76.1], to investigate the dependence of the web effectiveness factor  $\nu$  on the different parameters, among these the reinforcement details, the width of the beam web, and the concrete strength.

The main purpose of the fatigue tests was to determine the fatigue strength of beams with shear reinforcement designed in accordance with the web crushing criterion for the loading gap  $V_{\min} = 15$  kN and  $V_{\max}$  = the service load (50%-60% of the ultimate load).

The principal conclusions drawn from the tests are as follows:

- The results are generally in good agreement with the web crushing criterion, (eq. (1.1)-(1.2)). The best correspondence between test results and the theory are obtained for  $\nu = 0.70$  when all tests are considered. For the individual test series the closest fit are obtained with the  $\nu$ -values in the interval  $0.58 < \nu < 0.83$ ,
- The dependences of  $\nu$  on the concrete strength and the concrete cover were found to be significant. The best empirical model for  $\nu$  was

$$\nu = 1.11 \left( 0.8 - \frac{\sigma_c}{200} \right) \left( 1.0 - 1.2 \frac{e}{b} \right) \quad (1)$$

where  $\sigma_c$ ,  $e$  and  $b$  are the concrete strength, concrete cover and width of beam web, respectively. However, when test results from other laboratories are included, the more simple model

$$\nu = 0.8 - \frac{\sigma_c}{200} \quad (2)$$

are producing results quite as good as (1), why this model is recommended for practical use,

- The fatigue tests showed that with a maximum load not exceeding 56% of the ultimate load,  $2 \cdot 10^6$  pulsations did not lead to shear failure. A statical test after the  $2 \cdot 10^6$ -pulsations did not show any reduction of the load carrying capacity.

## RESUMÉ

Rapporten omhandler 40 statiske forsøg og 7 udmattelsesforsøg med simpelt understøttede T-bjælker belastet med de symmetrisk anbragte enkeltkræfter. Bjælkerne var forsynet med forskydningsarmering, i almindelighed i form af lodrette bøjler.

Formålet med de statiske forsøg var - udover at bekræfte resultaterne af tidligere forsøgsserier rapporteret i [76.1] - at undersøge effektivitetsfaktoren  $\nu$ 's afhængighed af forskellige parametre, bl.a. armeringsdetaljer, kropbredde og betonstyrke.

Udmattelsesforsøgenes hovedformål var at bestemme udmattelsesstyrken af bjælker med en forskydningsarmering dimensioneret efter trykbrudskriteriet for spændingsgab  $V_{\min} = 15 \text{ kN}$  og  $V_{\max} =$  brugslasten (dvs. 50-60% af brudlasten).

På basis af forsøgsresultaterne kan drages følgende hovedkonklusioner:

- Resultaterne er i god overensstemmelse med trykbrudskriteriet (ligning (1.1) - (1.2)). Den bedste overensstemmelse mellem forsøg og teori opnås med  $\nu = 0.70$ , når alle forsøgsresultater betragtes. For de enkelte forsøgsserier opnås den bedste overensstemmelse med  $\nu$ -værdier, der varierer inden for intervallet  $0.58 < \nu < 0.83$ ,
- Variation i effektivitetsfaktoren med betonstyrken og betondæklaget fandtes at være signifikant. Den bedste empiriske model for  $\nu$  som funktion af disse parametre var

$$\nu = 1.11 \left( 0.8 - \frac{\sigma_c}{200} \right) \left( 1.0 - 1.2 \frac{e}{b} \right) \quad (1)$$

hvor  $\sigma_c$ ,  $e$  og  $b$  angiver henholdsvis betonstyrken, betondæklagets tykkelse og kropbredden. Medtages imidlertid resultater fra andre laboratorier, giver den simplere model

$$\nu = 0.8 - \frac{\sigma_c}{200} \quad (2)$$

mindst lige så gode resultater som (1). Denne model anbefales derfor ved praktiske anvendelser,

- Udmattelsesforsøgene viste, at med en maksimumlast  $V_{\max}$  mindre end 56% af brudlasten fører  $2 \cdot 10^6$ -pulsation ikke til forskydningsbrud. Et statisk forsøg efter  $2 \cdot 10^6$ -pulsationer førte ikke til nogen reduktion i forskydningsbæreevnen.

<u>TABLE OF CONTENTS</u>	Page
INTRODUCTION .....	9
TABLES AND FIGURES .....	11
NOTATIONS .....	13
1. THEORETICAL BACKGROUND	
1.1 The web crushing criterion .....	15
1.2 Effective concrete strength .....	16
2. TEST PLANNING	
2.1 Results of series T.....	18
2.2 The purpose of the tests .....	19
2.3 Test beams .....	20
3. TEST EXECUTION	
3.1 Manufacturing and curing .....	29
3.2 Testing of concrete .....	32
3.3 Testing of stirrup reinforcement .....	32
3.4 Testing of longitudinal reinforcement .....	32
3.5 Testing of beams .....	35
4. TEST ANALYSIS, STATIC TESTS	
4.1 Computer programs .....	38
4.2 General behaviour .....	40
4.3 Loads, deflections and dial gauge readings .....	41
4.4 Stirrup strains and forces .....	41
4.5 Cracking and crack width .....	46
4.6 Ultimate loads .....	46
4.6.1 Results of all series .....	46
4.6.2 Results of the individual series .....	49
4.6.3 Results of tests with special beams .....	57
5. DISCUSSION AND CONCLUSIONS	
5.1 Failure mechanism .....	59
5.2 Strong shear reinforcement .....	63
5.3 Calculation of effectiveness factor .....	63



6.	FATIGUE TESTS	
6.1	Purpose of tests .....	73
6.2	Test beams .....	73
6.3	Testing of beams .....	74
6.4	Test results .....	75
6.4.1	Fatigue failures .....	75
6.4.2	Results of stirrup force measurements ....	80
6.5	Discussion and conclusions .....	82
	REFERENCES .....	84

## INTRODUCTION

Dating back to the Spring of 1973, a theoretical and experimental study of the shear strength of reinforced concrete beams has been carried out at the Structural Research Laboratory of the Technical University of Denmark. The project was sponsored by the Danish Council for Scientific and Technical Research which granted funds for three years of experimental investigation.

The main purpose of this test programme was to study an expression for the ultimate shear load based upon plastic analysis. The theory was originally proposed by Nielsen [67-1], [67-2] as a lower bound for the load-carrying capacity when web failure is critical. Later it was shown, Nielsen & Bræstrup [75-1], that the web crushing criterion is also an upper bound, thus establishing it as the correct plastic solution for the shear strength.

The first test series of this programme, the series T, consisting of 26 beams, is reported in Bræstrup et al. [76-1]. The purpose of the present paper is to report on the test series V, U, X, B and S, which include static tests with 40 beams and fatigue tests with 7 beams.

The report [76-1] contains a rather detailed description of the test procedure and equipment. In the present report, only the most essential information concerning these points is repeated. For further details, the reader is referred to [76-1].

The laboratory reports, photographs and computer output, corresponding to the individual beams, are filed at the Laboratory in unpublished appendices.

The first part of the document discusses the importance of maintaining accurate records of all transactions and activities. It emphasizes the need for transparency and accountability in financial reporting. The second part outlines the specific procedures and controls that should be implemented to ensure the integrity of the data. This includes regular audits, internal reviews, and the use of standardized reporting formats. The document also addresses the role of management in overseeing these processes and ensuring that they are effectively executed. Finally, it provides a summary of the key findings and recommendations for improving the overall financial management system.

The following table provides a detailed breakdown of the financial data for the period under review. It includes information on revenue, expenses, and net income, categorized by department and project. The data shows a steady increase in revenue over the period, which is primarily driven by the completion of several major projects. However, there has been a corresponding increase in expenses, particularly in the area of personnel and materials. The net income remains positive, indicating that the organization is operating profitably. The table also includes a comparison of the actual results against the budgeted figures, highlighting areas where the organization has exceeded or fallen short of expectations.

In addition to the financial data, the document also provides a detailed analysis of the operational performance of the organization. This includes information on the completion of projects, the efficiency of resource utilization, and the overall quality of the work. The analysis shows that the organization has made significant progress in completing its projects on time and within budget. However, there are still some areas where the organization is facing challenges, such as delays in the procurement of materials and the need for additional personnel. The document provides a list of recommendations for addressing these challenges and improving the overall operational performance.

The document concludes with a summary of the key findings and recommendations. It emphasizes the importance of maintaining accurate records and implementing robust controls to ensure the integrity of the financial data. It also highlights the need for management to oversee these processes and ensure that they are effectively executed. The document provides a list of specific recommendations for improving the financial management system, including the implementation of standardized reporting formats, the use of internal reviews, and the regular auditing of financial records. The document also provides a list of recommendations for improving the operational performance of the organization, including the need for better resource utilization and the implementation of project management best practices.

The document is intended to provide a comprehensive overview of the financial and operational performance of the organization. It is intended to be used by management and other stakeholders to make informed decisions about the organization's future. The document provides a clear and concise summary of the key findings and recommendations, and it is intended to be a valuable resource for anyone involved in the organization's financial and operational management.

TABLES AND FIGURES

The tables and figures are numbered consecutively within each main section. Below they are listed with page numbers for easy reference.

Tables

2.1	Data of test beams.....	22
2.2	Series characteristics.....	26
3.1	Concrete recipes.....	30
3.2	Concrete test results.....	33
3.3	Tension test results for stirrup reinforcement.....	34
3.4	Tension test results for longitudinal reinforcement.....	35
4.1	Strength properties of test beams.....	39
4.2	Deflexions at service load.....	42
4.3	Recording of stirrup yield.....	45
4.4	Test results from all static tests.....	47
4.5	Average v-values of the test series.....	56
5.1	Average v-values compared to the expression $v = \frac{nod}{b}$ .....	65
5.2	Average v-values compared to the empirical expression $v = 1.11 \left( 0.8 - \frac{c}{200} \right) \left( 1.0 - 1.2 \frac{e}{b} \right)$ .....	70
5.3	Average v-values of other test series.....	72
6.1	Results of fatigue tests .....	73
6.2	Results of fatigue tests .....	75
6.3	Stirrup stresses at $V_{max}$ and measured and calculated number of pulsations .....	82

Figures

1.1	Illustration of effective shear depths .....	17
2.1	Test results for series T52, T60 and T90 .....	19
2.2	Normal sections of test beams .....	23-24
2.3	Elevation .....	25
2.4	Reinforcement details of beam No.R4251 .....	25
2.5	Expected shear and flexural strength of test beams .....	26-28

3.1	Grading curves for fine and coarse aggregate ..	31
3.2	Loading diagram and position of gauge stirrups and dial gauges .....	36
3.3	Overall view of beam test rig .....	36
4.0	Structure of computer program for analysis of data from beam tests .....	38
4.1	Stirrup force curves for Beam No.U6007 .....	43
4.2	Maximum recorded stirrup force versus the reinforcement degree, $\psi$ .....	44
4.3	Stirrup force curves for Beam No.X9018 .....	44
4.4	Results of all shear tests .....	48
4.5	Results of all shear tests inclusive series T .	48
4.6	Results of series V .....	50
4.7	Results of series U .....	50
4.8	Results of series Uc .....	51
4.9	Results of series Uh .....	51
4.10	Results of series Um .....	52
4.11	Results of series X .....	52
4.12	Results of series Xd .....	53
4.13	Results of series B .....	53
4.14	Results of series Bd .....	54
4.15	Results of series SPB .....	54
4.16	Results of series S .....	55
4.17	The $v$ -dependence of the concrete strength .....	58
5.1	Typical failures for each series .....	60
5.2	Shear failure of Beam No.U6007c .....	61
5.3	Normal sections of the Beams U6017, U6017c, and U6017h .....	62
5.4	Web failure mechanism .....	65
5.5	Web failure mechanism .....	66
5.6	The average $v$ -values compared to the empirical expression $v = 0.84 - 1.0 e/b$ .....	68
5.7	The average $v$ -values compared to the empirical expression $v = 0.8 - \sigma_c/200$ .....	70
5.8	The average $v$ -values of own and others' test series compared to the empirical model $v = 0.8 - \sigma_c/200$ .....	71
6.1	Test rig .....	74
6.2	Fatigue failure of stirrups. $V_{max} = 0.5 V_u$ .....	76
6.3	Fatigue failure of concrete struts. $V_{max} = 0.76 V_u$ .....	76
6.4	Fatigue failure of concrete struts. $V_{max} = 0.74 V_u$ .....	77
6.5	Fatigue failure of stirrups. $V_{max} = 0.62 V_u$ .....	77
6.6	Fatigue failure of main reinforcement bars. $V_{max} = 0.69 V_u$ .....	78
6.7	Fatigue failure of stirrups. $V_{max} = 0.56 V_u$ .....	79
6.8	Development of the cracks during the fatigue test of Beam No.5610p .....	79
6.9	Stirrup force measurements .....	81
6.10	Stirrup force measurements .....	81
6.11	Wöhler-diagram .....	83

NOTATIONS

The symbols are defined when they first occur in the test. The frequently used notations are listed alphabetically below.

- b : Web width
- $b_s$  : Interior width of stirrup hoops
- $b_o$  : Flange width
- d : Diameter of tensile reinforcement
- e : Concrete cover
- $E_s$  : Elastic force-strain modulus for steel bar
- h : Beam depth
- $h_s$  : Depth of web from the bottom of flange to the centroid of lower layer of main reinforcement
- $h_w$  : Depth of web measured from bottom of flange to the centroid of main reinforcement
- $h_o$  : Flange depth
- $h^*$  : Effective shear depth
- $k_1, k_2$  : Constants
- N : Number of tests in a series (sample)
- n : Number of tensile reinforcement bars supported by stirrup bends
- n : Number of pulsations
- $P_a$  : Force in stirrups
- $P_y$  : Yield force of stirrups
- s : Equivalent stirrup stress. Standard deviation based upon (N-1) degrees of freedom
- $s_y$  : Equivalent stirrup yield stress

V : Applied shear load  
V<sub>cr</sub> : Shear cracking load  
V<sub>F</sub> : Flexural failure load  
V<sub>u</sub> : Ultimate shear load  
z : Internal moment lever arm

---

$\alpha$  : Stirrup inclination  
 $\beta$  : Stress concentration factor  
 $\theta$  : Inclination of yield lines  
v : Web effectiveness ratio  
 $\bar{v}$  : Average web effectiveness factor of a test series  
 $\sigma_b$  : Compressive concrete strength  
 $\sigma_c$  : Compressive concrete cylinder strength  
 $\sigma_c^*$  : Effective web strength  
 $\sigma_t$  : Tensile concrete strength  
 $\sigma_{u+}$  : Maximum stress in stirrup during pulsation  
 $\sigma_y$  : Yield stress of stirrup steel  
 $\tau$  : Nominal shear stress of beam  
 $\psi$  : Mechanical degree of shear reinforcement

## 1. THEORETICAL BACKGROUND

### 1.1 The Web Crushing Criterion

The theoretical background for the test series is an analysis based upon the theory of plasticity. The theory is described in the references [67-1], [75-1], [77-1], [78-1], [78-2]. Only the solutions for simply supported beams with concentrated loads are given here.

The load-carrying capacity of beams with vertical stirrups is given by the web crushing criterion

$$V = bh^* s_y \sqrt{\frac{\sigma_c^*}{s_y} - 1} \quad \text{for } s_y \leq \frac{1}{2} \sigma_c^* \quad (1.1a)$$

$$V = \frac{1}{2} bh^* \sigma_c^* \quad \text{for } s_y \geq \frac{1}{2} \sigma_c^* \quad (1.1b)$$

Here:

- V is the applied shear force.
- b is the width of the web.
- h\* is the effective shear depth.
- s<sub>y</sub> is the equivalent reinforcement strength, i.e. the stress equal to the yield force in the stirrups per unit area perpendicular to the stirrups.
- σ<sub>c</sub>\* is the effective compressive strength of the concrete.  
σ<sub>c</sub>\* = vσ<sub>c</sub>.
- σ<sub>c</sub> is the cylinder strength.
- v is the web effectiveness parameter.

The equations (1) may be stated on non-dimensional form as

$$\tau/\sigma_c = \sqrt{\psi(v - \psi)} \quad \psi \leq v/2 \quad (1.2a)$$

$$\tau/\sigma_c = v/2 \quad \psi \geq v/2 \quad (1.2b)$$



where we have introduced the nominal shear stress  $\tau$  and the mechanical shear reinforcement degree  $\psi$ :

$$\tau = \frac{V}{bh^*} \quad , \quad \psi = \frac{s_y}{\sigma_c}$$

The load-carrying capacity of beams with inclined stirrups, on non-dimensional form, is given by the web crushing criterion:

$$\tau/\sigma_c = \sqrt{\psi \sin^2 \alpha (v - \psi \sin^2 \alpha) + \psi \cos \alpha \sin \alpha} \quad , \quad (1.3a)$$
$$\psi \sin^2 \alpha \leq \frac{1}{2} v(1 + \cos \alpha)$$

$$\tau/\sigma_c = \frac{1}{2} v \cot \frac{\alpha}{2} \quad , \quad \psi \sin^2 \alpha > \frac{1}{2} v(1 + \cos \alpha) \quad (1.3b)$$

$\alpha$  is the stirrup inclination.

## 1.2 Effective Concrete Strength

In order to be able to use the equations (1.1)-(1.3) for analysis and design, we need to assess the values of the quantities  $v$  and  $h^*$ .

There are two main reasons why the web effectiveness ratio  $v$  must be less than unity. Firstly, because of the limited deformability of the concrete and the unstable nature of the concrete failure, we cannot expect the concrete stress to equal the maximum compressive strength at all points of the yield lines at failure. Secondly, the fact that the compression is applied to the web concrete through the longitudinal bars. This concentration of the load leads to failure of the concrete at a stress level which, as an average over the web, is less than the cylinder strength.

There are probably several other minor reasons. For instance, the web strength might also depend on the stirrup spacing in the

longitudinal direction. Furthermore, the effective strength of the web decreases because of cracks developed in early loading stages and having another direction than the final cracks.

An assessment of the web effectiveness parameter  $v$ , by comparing the formulas for the load-carrying capacity with experimental results from shear tests, is influenced by the choice of effective shear depth  $h^*$ . The depth  $h^*$  is the distance between the tension and compression stringers. For T - beams, we may take the latter as being identical to the compression flange, but even so, there are a number of ways of defining the shear depth, as illustrated in Fig. 1.1. The usual practice is to relate the nominal shear stress to the effective depth  $d$ . The Danish Code of Practice puts the shear depth equal to the internal moment lever arm  $z$ .

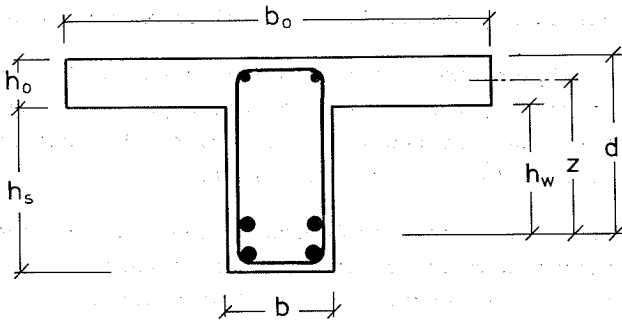


Fig. 1.1 Illustration of effective shear depth

## 2. TEST PLANNING

### 2.1 Results of Series T

The results of the first test series (series T) in this test programme are reported in [76.1]. The principal results of this series are summarized below:

1. The behaviour of the beams under loading to failure is essentially as predicted by the theory. A marked decrease in the inclination of newly formed cracks is observed as the load increases. At yield, the deformation consists of a vertical translation of the load section relative to the support section.
2. No significant difference is observed between the ultimate shear load of beams with different strength of main reinforcement.
3. Beams with very strong stirrup reinforcement,  $\psi > 1/2 v$ , achieved approximately identical ultimate loads.
4. An analysis shows that  $h^* = z$  is a reasonable choice. With this choice, the web effectiveness parameter giving closest fit to the test results is  $v = 0,74$  (the coefficient of variation is 7,4%, see Fig. 2.1).

The result that  $v$  does not depend on the yield strength of the main reinforcement is utilized in the planning of the tests described in this report. The yield strength of the main reinforcement is not considered an influential parameter, i.e. this parameter can be varied at the same time as a presumed influential parameter (e.g. the diameter of the main reinforcement is varied).

The choice of  $h^*$  is not discussed further in this report. With reference to the results of series T,  $h^*$  is always taken as being equal to the internal moment lever arm  $z$  in the following.

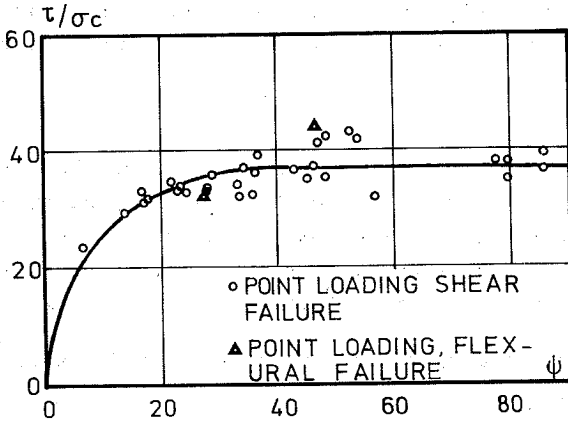


Fig. 2.1 Test results for series T52, T60, and T90 (shear depth =  $h^* = z$ )

## 2.2 Purpose of the Tests.

The main purposes of the test series considered in this report were:

1. To confirm the results of the previous test series reported in [76.1].
2. To investigate the hypothesis that  $v$  is less than unity because of the stress concentration above the tensile reinforcing bars by determining the dependence of  $v$  on a) the main reinforcement details (i.e. diameter of bars, concrete cover and stirrup layout), b) the width of the beam web.
3. To obtain an indication of the influence of the concrete strength and stirrup inclination by means of a few pilot tests.

4. To test the fatigue strength of beams with shear reinforcement designed in accordance with the web crushing criterion.

### 2.3 Test Beams.

Each beam is denoted by a beam number, e.g. U6007c, consisting of a series identification (the letters), a specimen number which furnishes information on the nominal yield strength of the main reinforcing bars in  $\text{kp/mm}^2$  (first two digits) and nominal shear reinforcement degree  $\psi$  in  $10^{-2}$  (the last two digits).

The data of the individual beams is given in Table 2.1, Fig. 2.2 and Fig. 2.3.

Table 2.1 contains all the information concerning the type and amount of shear and main reinforcement, the reinforcement details and sectional geometry, the nominal concrete strength and the nominal flexural failure load.

Fig. 2.2a-1 shows normal sections and Fig. 2.3 the elevation of the test beams.

The characteristic data of the beams in a series can be found in Table 2.1 and in Fig. 2.2, but is more clearly shown in Table 2.2.

As can be seen from the table, and as mentioned in Sec. 2.2, the purpose of these test series was to investigate the influence on the shear capacity of different parameters and among these the reinforcement details. The point was further studied by a few pilot tests collected in series SPB, consisting of the beams with Nos. 5617c, R4251, R5651t and U5604p.

In the beam No. U5617c, the tensile reinforcement was not placed in the stirrup bends (see Fig. 2.2i).

Beam No. R4251 had a steel plate as tensile reinforcement with the stirrups welded to the plate (Fig. 2.2k and Fig. 2.4). Because of

the welding, the stirrups were placed singly at close intervals ( $a = 52.5$  mm).

Beam No. R5651t, with an ordinary tensile reinforcement and with shear reinforcement as R4251, served as a reference beam.

The last beam of series SPB was planned as a beam belonging to the series of fatigue tests (see Section 6), but since  $2 \cdot 10^6$  pulsation did not destroy the beam, it was subjected to a static test to study the influence of the pulsations on the static behaviour of the beam.

The nominal shear reinforcement for the beams in the individual series is marked on Fig.2.5 where the maximum shear stress (i.e. the shear stress corresponding to the nominal flexural failure load) and the shear strength calculated from equation (1.2) on the basis of expected  $v$ -values are also indicated.

Series	Beam No.	Stirrup reinforcement	Nominal concrete strength MPa	Tensile reinforcement			Compress. reinforcement			Reinforcement details (see fig. 2.2)	Geometry of cross-section in mm (see fig. 2.2)				Nominal flexural strength P <sub>F</sub> (kN)	
				Number of bars	Diam (mm)	Steel quality	Number of bars	Diam (mm)	Steel quality		b	d	d <sub>0</sub>	z		
v	V6002 E W V6004 E	2R6/210 2R6/131	35.0	4	25	SKS60	2	12	FKF42	a	200	343	31	298	362	
U	U6002 E W U6004 E W U6007 E W U6010 E W U6017 E W U6025 E	R6/210 2R6/210 2R6/131 2R6/96 2R10/175 2R10/105	20.0	4	25	SKS60	2	12	FKF42	a	200	343	31	298	350	
U <sub>c</sub>	U6007cE W U6010cE W U6013cE W U6017cE W U6023cE W U6029cE W U6044cE W	2R6/131 2R6/96 2R6/96 2R10/175 2R10/131 2R10/105 2S10/117	20.0	4	25	SKS60	2	12	FKF42	b	200	343	31	298	350	
U <sub>h</sub>	U6007hE W U6010hE W U6017hE W	2R6/131 2R6/96 2R10/175	20.0	4	25	SKS60	2	12	FKF42	c	200	343	31	298	350	
U <sub>m</sub>	U4213mE W U4222mE W U4230mE W U4244mE W	2R10/210 2R10/117 2S10/175 2S10/117	20.0	4	35	FKF42	2	12	FKF42	d	200	340	31	295	476	
X	X6009 E W X6018 E W X9032 E W X9043 E W	2R6/210 2R6/105 2R10/175 2R10/131	10.0	8	12	SKS90	4	12	FKF42	f e f e f e	200	358 353 349 349		313 308 304 304	172 229 285 285	
B	B6009 E W B9018 E W B9025 E W B9025aE W B9029 E W B9040 E W	2R7/175 2R10/150 2R10/105 2R10/105 2R10/89 2S10/131	10.0	8 6 6 8 8 9	16	SKS60 SKS90 SKS90 SKS90 SKS90 SKS90 <sup>3)</sup>	4 2 2 4 4 4	16 12 12 16 16 16	SKS60 FKF42 FKF42 SKS60 <sup>2)</sup> SKS60 SKS60	h g g <sup>1)</sup> g <sup>1)</sup> g g h g h		380	354	33 31 31 33 33 33	309	250 300 300 413 413 413
SPB	U5617L E W U5604pE W R4251 E W R5651 E W	2R10/175 R10/87.5 2R6/210 R10/52.5 R10/52.5	20.0 10.0 10.0	4 4 8	25 16 16	SKS56 SKS56 SKS56	2 2 3	12 12 16	FKF42 FKF42 SKS52 SKS52	i k a j	200	345 345 359 359	31 31 33 33	300 300 314 314	328 328 340 278	
S	S9013 E W S9039 E W S9040 E W S9050 E W	2R7/210 <sup>4)</sup> 2R10/131 <sup>4)</sup> 2R10/131 <sup>4)</sup> 2R10/105 <sup>4)</sup>	10.0	8 10 10 10	12	SKS90	4	16	FKF42 FLF42 SKS52 SKS52	l l l l	200	35	33	310	249 310 310 310	
FT	U5604pE W U5606pE W U5606qE W U5606rE W U5606sE W U5610pE W T6007pE W	2R6/210 2R7/210 R7/105 2R7/210 R7/105 2R7/210 R7/105 2R7/210 R7/105 2R6/96 R7/210	20.0 20.0 20.0 20.0 20.0 20.0 20.0 20.0 20.0 10.0	4 4 4 4 4 4 4 4 4 4 6	16 25 25 25 25 25 25 25 25 25	SKS56 SKS56 SKS56 SKS56 SKS56 SKS56 SKS56 SKS56 SKS56 SKS56 SKS60	2 2 2 2 2 2 2 2 2	12 12 12 12 12 12 12 12 12	FKF42 FKF42 FKF42 FKF42 FKF42 FKF42 FKF42 FKF42 FKF42 FKF42 SKS60	a a a a a a a a a a j	200	345 345 345 345 345 345 345 345 345 345 354	31 31 31 31 31 31 31 31 31 31	300 300 300 300 300 300 300 300 300 300 290	328 328 328 328 328 328 328 328 328 328 290	

1) The tensile reinforcement was only 6 K16  
 2) The tensile reinforcement was curtailed just before the support in EAST  
 3) 5 bars in the bottom layer  
 4) 45°-inclined stirrups

Table 2.1 Data of test beams

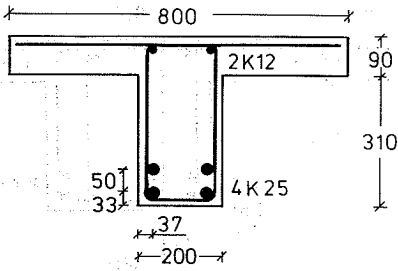


Fig. 2.2a Series V, U

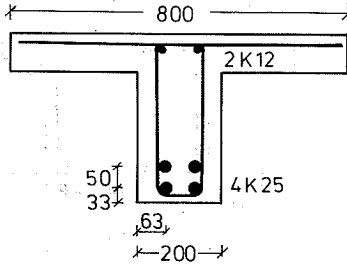


Fig. 2.2b Series Uc

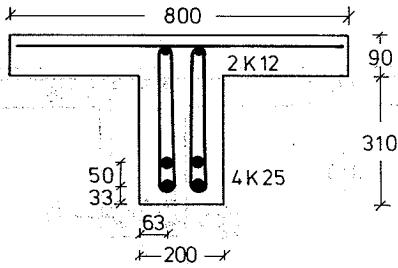


Fig. 2.2c Series Uh

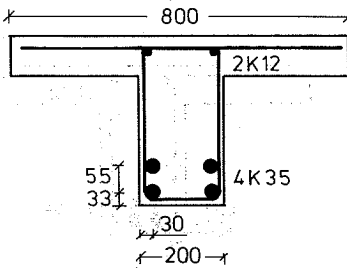


Fig. 2.2d Series Um

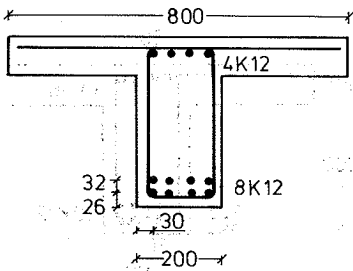


Fig. 2.2e Series X

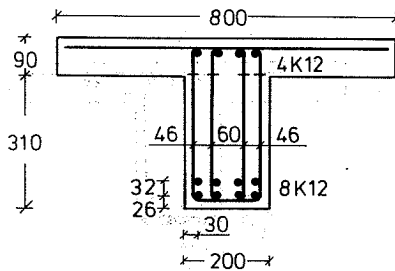


Fig. 2.2f Series Xd



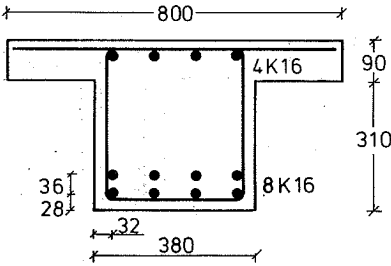


Fig. 2.2g Series B

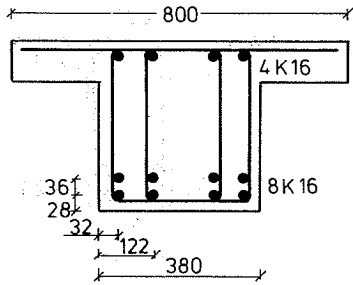


Fig. 2.2h Series Bd

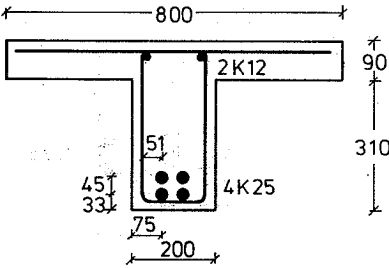


Fig. 2.2i Beam U5617i

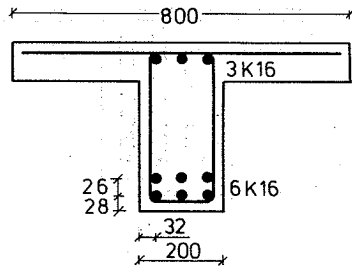


Fig. 2.2j Beam R5651t

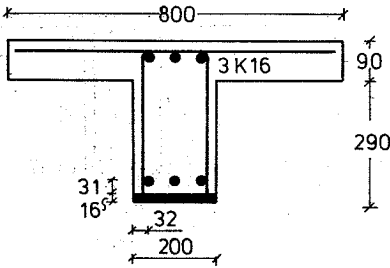


Fig. 2.2k Beam R4251

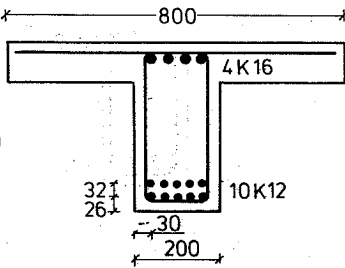


Fig. 2.2l Series S

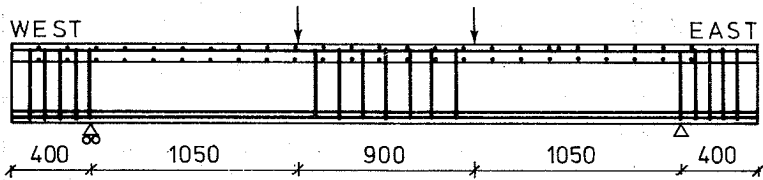


Fig. 2.3 Elevation of test beam. Variable shear reinforcement not shown.

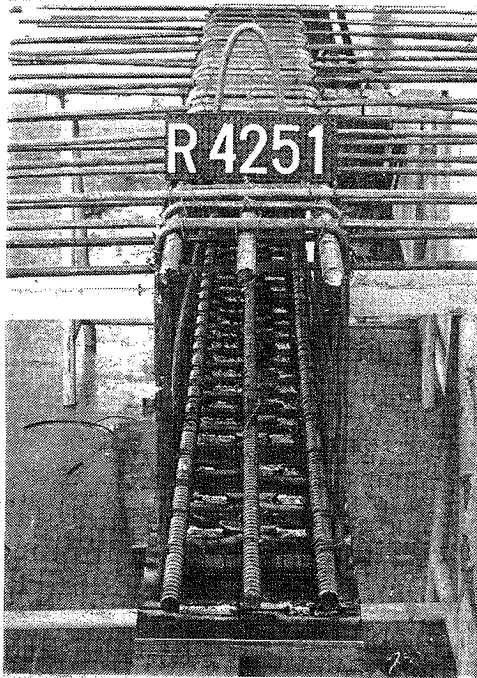


Fig. 2.4 Reinforcement details of Beam No. R4251.

Serie	Stirrup arrangement	Nominal concrete strength $\sigma_c$ (MPa)	Diameter of tensile reinf. $d$ (mm)	Concrete cover $e$ (mm)	Beam width $b$ (mm)	Stirrup inclination $\alpha$ (°)
V		35,0	25	24	200	90
U		20,0	25	24	200	90
Uc		20,0	25	50	200	90
Uh		20,0	25	50	200	90
Um		20,0	35	12	200	90
X		10,0	12	24	200	90
x <sub>d</sub>						
B		10,0	16	24	380	90
B <sub>d</sub>						
S		10,0	12	24	200	45
U <sub>p**</sub>		20,0	25	24	200	90

Table 2.2 Series characteristics

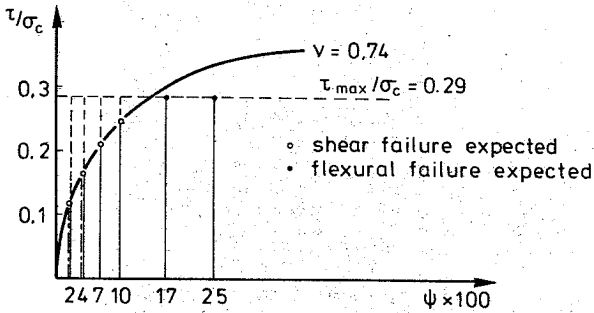


Fig. 2.5a Expected strength. Series V and U

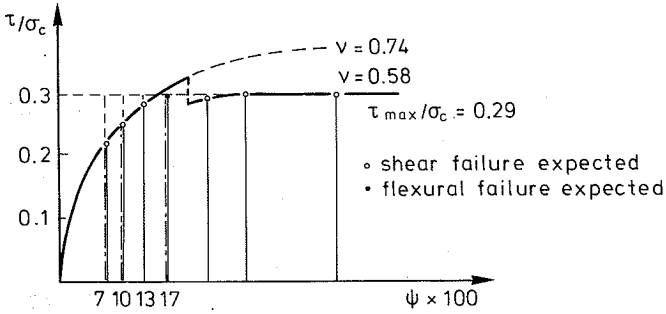


Fig. 2.5b Expected strength. Series Uc and Uh

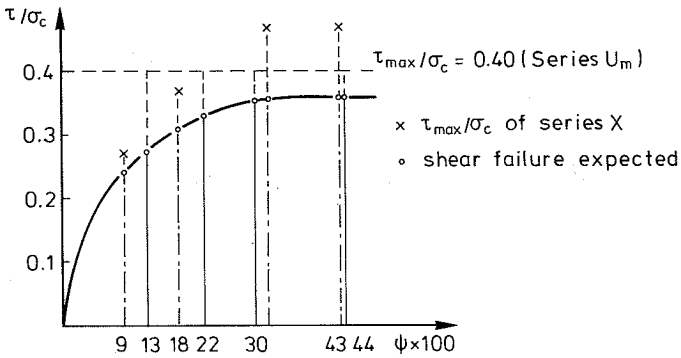


Fig. 2.5c Expected strength. Series Um and X

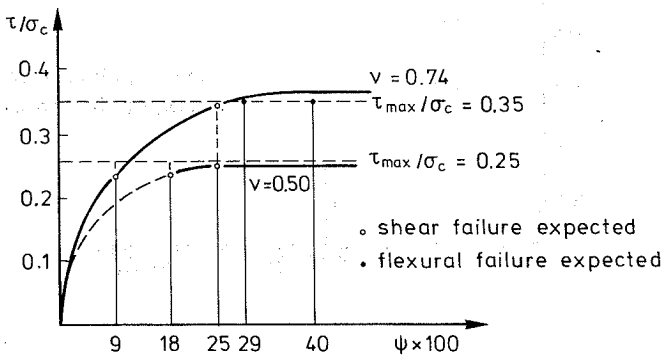


Fig. 2.5d Expected strength. Series B. (Since B9018 and B9025 had flexural failure, the flexural strength of the other beams in the series was improved).

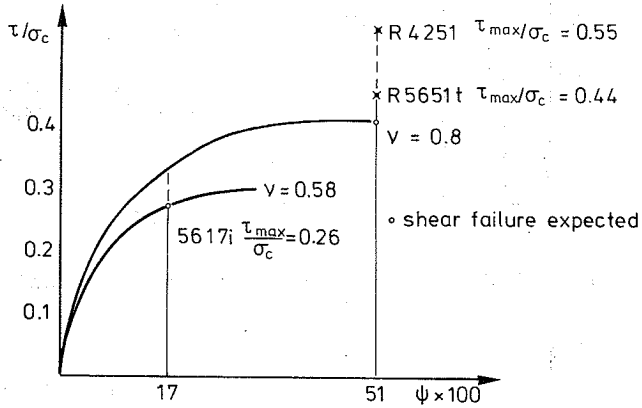


Fig. 2.5e Expected strength. Series SPB.

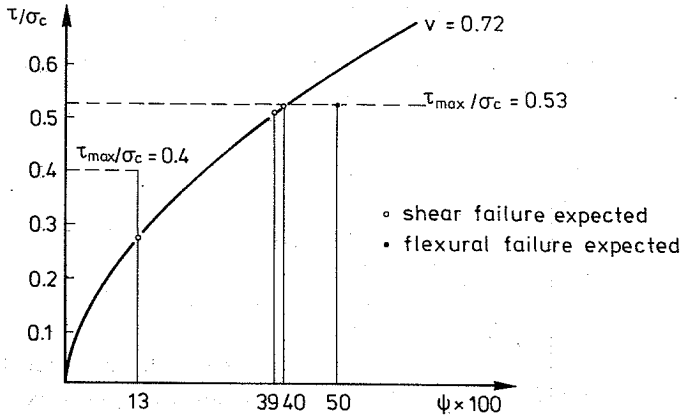


Fig. 2.5f Expected strength. Series S.

### 3. TEST EXECUTION

#### 3.1 Manufacture and Curing

The steel for the main reinforcement was hot-rolled, deformed bars of Swedish fabrication (SKS52, SKS60 and SKS90) or Danish fabrication (FKF42).

Most beams had shear reinforcement of mild steel (St37) in smooth bars with a diameter of 6 mm (R6), 7 mm (R7) or 10 mm (R10). A few beams with strong shear reinforcement had stirrups of cold-drawn Swedish steel (Ss50), in smooth bars with a diameter of 10 mm (S10).

The exact amount and type of reinforcement in every beam is given in Table 2.1.

The individual bars, delivered in lengths of 8 to 14 m were numbered and distributed in the test beams. A table of the distribution of the bars in the beams is to be found in Appendix A.

As flange reinforcement and as stirrups in the anchorage zones and in the bending span, smooth, mild steel with a diameter of 8 mm was used. The amount of this reinforcement is shown in Fig. 2.3. Design of the flange reinforcement is included in [76.1], sec. 2.4.

The beams were cast in steel moulds together with 9 - 12 companion cylinders.

Three batches (four batches for series B) of concrete were used for each beam. The composition of the batches of each beam is given in Table 3.1, together with the average strength of the cylinders from the batch and the number of days from casting to testing.

The cement was portland cement, type "rapid". The aggregate was sea material. Typical grading curves for gravel (0 - 8 mm) and stone (8 - 32 mm) are shown in Fig. 3.1.

Beam No.	Water kg	Cement kg	Gravel kg	Stone kg	Concrete Strength $c_c$ (MPa)	Number of days from curing to testing
V6002	34.4	54.7	156	209	35.7	14
V6004	34.4	54.7	156	209	36.4	14
U6002	34.4	32.0	139	245	19.6	14
U6004	35.4	33.0	143	253	21.1	14
U6007	34.9	32.5	184	206	14.7	14
U6010	34.9	32.5	184	206	16.5	21
U6017	34.9	32.5	184	206	20.1	28
U6025	34.5	36.2	183	204	20.2	14
U6007c	34.9	32.5	184	206	18.3	14
U6010c	33.5	33.5	185	207	19.3	14
U6013c	34.9	32.5	184	206	12.4	14
U6017c	34.5	36.2	183	204	18.4	14
U6023c	34.5	36.2	183	204	17.2	28
U6029c	34.5	36.2	183	204	20.0	28
U6044c	34.5	36.2	183	204	15.0	14
U6007h	33.9	32.5	184	206	15.5	14
U6010h	33.5	33.5	185	207	17.9	17
U6017h	34.5	36.2	183	204	20.3	14
U4213m	34.5	36.2	183	204	14.2	14
U4222m	34.5	36.2	183	204	15.7	14
U4230m	34.5	36.2	183	204	16.8	14
U4244m	34.5	36.2	183	204	16.5	14
X6009	34.4	27.2	193	194	7.3	14
X6018	34.4	28.0	193	194	9.4	14
X9032	34.4	28.0	193	194	8.5	14
X9043	34.4	28.0	193	194	8.3	14
B6009	35.0	29.0	199	200	I 11.2 II 11.9 III 10.3 IV 9.5	14
B9018	35.0	29.0	199	200	10.1	15
B9025	35.0	29.0	199	200	11.0	14
B9025a	35.0	29.0	199	200	12.3	14
B9029	35.0	28.5	199	200	I 11.0 II 9.7 III 9.6 IV 8.7	19
B904c	35.0	28.5	199	200	I 7.8 II 8.6 III 9.4 IV 9.0	21
U5617a	33.7	36.5	185	206	I 20.5 II 17.4 III 16.5 x 17.2	15
U5604p	33.0	36.8	181	202	I 22.7 II 24.1	15 21
R4251	35.0	29.0	199	200	I 9.6 II 10.4 III 11.4	18
R5651	35.0	30.0	199	200	I 9.3 II 9.2 III 8.1	23
S9013	35.0	29.0	199	200	I 9.4 II 8.5 III 9.1	15
S9039	35.0	30.0	199	200	I 11.5 II 12.0 III 11.3	29
S9040	35.0	29.0	199	200	I 7.8 II 7.5 III 7.4	16
S9050	35.0	29.0	199	200	I 8.2 II 8.9 III 10.2	28
U5604p	33.0	36.8	181	202	I 22.7 II 24.1	15 21
U5606p	34.0	36.5	185	206	I 20.8 II 17.7 III 17.1 x 17.0	14
U5606q	34.0	36.0	185	206	I 21.0 II 21.2 III 19.5 x 19.2	35
U5606r	34.0	36.5	185	206	I 19.6 II 15.9 III 19.5 x 14.6	30
U5606s	34.0	36.5	185	206	I 20.2 II 18.8 III 17.8	30
U5610p	33.6	32.6	182	203	17.4	21
T6007p	34	27.5	193	194	13.5	32

Table 3.1 Recipe

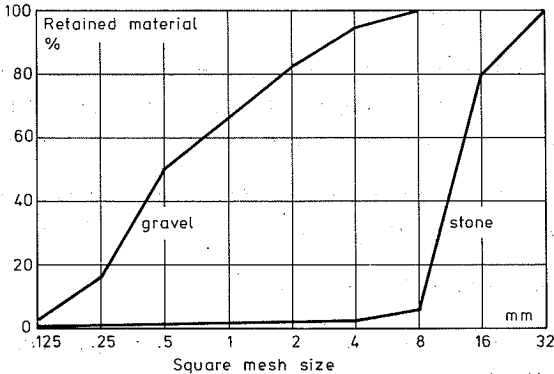


Fig. 3.1 Grading curves for fine and coarse aggregate.

The concrete of the beam was compacted by compressed air vibrators, whereas the cylinder moulds were fixed to a vibrating table. Beams and cylinders were cured together over a period of four days under wet burlap sacks at a temperature of approximately 20°C. The moulds were stripped two days after casting. Testing usually took place after 14 days (see Table 3.1).

The value for the concrete strength in Table 3.1 is to be understood as follows: The values with indication I to IV are the average strength of cylinders from the 1st., 2nd., 3rd. and 4th batches respectively. No indication, or the indication x, means that the cylinders were filled 1/4 (1/3) from each batch.

In the latter case, concrete in the shear zones is blended in the same way. In the first case, only concrete from one batch (usually the first) is placed in the shear zones.



### 3.2 Testing of Concrete

The concrete cylinders with a length of 300 mm and diameter 150 mm were tested in a 2000 kN compression test machine. Discs of soft fibreboard were placed between the specimen and the test machine.

The rate of loading during compression tests corresponded to approximately 1,5 MPa per minute.

Test results are given in Table 3.2.

The tensile strength was determined by split cylinder tests on four or five cylinders per beam.

### 3.3 Testing of Stirrup Reinforcement

The specimens were tested in a MOHR - FEDERHAFF 600 kN tension machine. The rate of loading to yield was approximately 200 N/sec., 500 N/sec. and 500 N/sec. for R6 - 7, R10 and S10 respectively.

On the basis of these test results, all given in Appendix A, the average stirrup strength,  $P_y$ , and the average force - strain modulus,  $E_s$ , can be found for each shear span. (See Table 3.3).

### 3.4. Testing of Longitudinal Reinforcement

The specimens of the longitudinal reinforcement were also tested in the MOHR - FEDERHAFF 600 kN tension machine. The rate of loading corresponded to 10 MPa per second.

All test results are collected in Appendix A.

Because of the small scatter, the longitudinal steel was not tested systematically. Only 5 to 15 tests were performed for each steel quality. The average values and scatter for each steel quality are given in Table 3.4.

Beam No.	Compression tests			Tension tests		
	N	$\sigma_c$ (MPa)	s (MPa)	N	$\sigma_c$ (MPa)	s (MPa)
V6002	5	35.7	0.81	5	3.0	0.25
V6004	5	36.4	0.68	5	3.5	0.68
U6002	5	19.5	0.64	3	1.8	0.52
U6004	5	21.1	0.18	5	2.3	0.19
U6007	5	14.7	0.26	5	1.6	0.29
U6010	5	16.5	0.87	4	1.8	0.16
U6017	5	20.1	0.32	4	2.1	0.27
U6025	5	20.2	0.91	5	2.4	0.21
U6007c	5	18.3	0.87	5	1.8	0.29
U6010c	5	19.3	1.10	5	2.1	0.35
U6013c	5	12.4	0.97	5	1.3	0.17
U6017c	5	18.4	0.81	5	2.2	0.28
U6023c	5	17.2	1.14	5	1.6	0.16
U6029c	5	20.0	0.51	5	1.8	0.22
U6044c	5	15.1	0.47	5	1.6	0.24
U6007h	5	15.5	0.96	5	1.7	0.12
U6010h	5	17.9	0.48	5	1.9	0.23
U6017h	5	20.3	0.83	5	2.1	0.09
U4213m	5	14.2	0.60	5	1.5	0.15
U4222m	5	15.8	1.39	4	1.7	0.31
U4230m	5	16.8	0.84	5	1.6	0.25
U4244m	5	16.5	0.61	5	1.6	0.16
X6009	5	7.3	0.50	4	0.9	0.08
X6018	5	9.4	0.44	5	1.3	0.05
X9032	5	8.5	0.63	5	0.9	0.11
X9043	5	8.2	0.29	5	0.9	0.09
B9009	12	10.7	1.04			
B9018	5	10.1	0.23	5	1.3	0.19
B9025	5	11.0	0.45	4	1.3	0.08
B9025a	4	12.3	0.55	5	1.3	0.16
B9029	12	9.7	0.94			
B9040	12	8.6	0.67			
U5617i	12	17.9	1.70			
U5604p	4	24.1	0.85			
R4251	5	9.6	0.38			
R5651t	4	9.3	0.18			
S9013	5	9.4	0.32			
S9039	5	11.5	0.39			
S9040	5	7.8	0.33			
S9050	3	8.2	0.52			
U5604p	4	24.1	0.85			
U5606p	9	18.5	1.72			
U5606q	9	20.6	1.02			
U5606r	9	16.4	2.64			
U5606s	4	20.2	0.77			
U5610p	5	17.4	0.94			
T6007p	10	13.5	0.84			

Table 3.2 Concrete test results

Beam no.	Stirrup steel	Yield force of stirrups $P_y$ (kN)	Force-strain modulus $E_s$ (MN)
V6002	W E R6	9.03	5.88
V6004	W E R6	9.03	5.88
U6002	W E R6	9.03	5.88
U6004	W E R6	9.03	5.88 6.06
U6007	W E R6	9.03	5.88
U6010	W E R6	9.03	5.88
U6017	W E R10	22.00 27.40	16.30 15.70
U6025	W E R10	22.70 26.95	16.30 16.70
U6007c	W E R6	9.67	6.06
U6010c	W E R6	9.67	6.06
U6013c	W E R6	9.67	6.06
U6017c	W E R10	29.00 30.50	16.00 16.70
U6023c	W E R10	25.80	16.70
U6029c	W E R10	25.40	16.10
U6044c	W E S10	50.00	18.20
U6007h	W E R6	9.67	6.06
U6010h	W E R6	9.67	6.06
U6017h	W E R10	29.15	16.10
U4213m	W E R10	29.50 29.80	16.10 16.70
U4222m	W E R10	29.70 29.75	16.10
U4230m	W E S10	55.80	19.05
U4244m	W E S10	51.30	18.50
X6009	W E R6	9.67	6.06
X6018	W E R6	9.67	6.06
X9032	W E R10	26.00 27.00	16.70
X9043	W E R10	26.65 26.60	16.10
B9009	W E R7	14.45 13.35	8.35 8.15
B9018	W E R10	26.65 27.20	16.70
B9025	W E R10	31.50 31.35	16.70
B9025a	W E R10	26.60 29.00	16.12
B9029	W E R10	26.10 24.00	16.12
B9040	W E S10	52.00	18.27
U5617l	W E R10	25.50 23.50	16.12
U5604p	W E R10	11.00 11.00	6.06
R4251	W E R10	24.30 23.65	16.70
R5651t	W E R10	23.35 22.45	17.25
S9013	W E R7	14.40 14.15	8.15
S9039	W E R10	24.50	17.25
S9040	W E R10	22.25 24.05	16.70
S9050	W E R10	23.65 23.00	17.25
U5604p	W E R6	11.00 11.00	6.06
U5606p	W E R7	13.60 14.50	8.35
U5606q	W E R7	14.80 14.05	8.00
U5606r	W E R7	13.40 14.50	8.00
U5606s	W E R7	14.85 13.90	8.35 8.15
U5610p	W E R6	10.45 10.65	6.06
T6007p	W E R7	13.80 14.60	8.35

Table 3.3 Tensile test results for stirrup reinforcement

Type of steel	Diameter	Number of tests	Average strength $\sigma$ (MPa)	Standard deviation s (MPa)
SKS 90	16	14	928.0	4.9
SKS 90	12	7	924.0	4.7
SKS 60	25	10	654.0	5.9
SKS 60	16	12	704.5	19.9
SKS 60	12	6	650.0	4.4
SKS 56	25	4	716.5	17.3
SKS 56	16	6	641.5	2.4
SKS 52	16	16	560.5	2.9
FKF 42	35	6	450.5	7.4
FKF 42	16	12	482.0	5.3
FKF 42	12	4	457.0	10.8
FKF 42	10	2	449.0	2.7

Table 3.4 Tension test results for longitudinal reinforcement.

### 3.5 Testing of Beams

Detailed descriptions of the test rig, test procedure and measuring equipment is given in [76.1]. Only the most necessary information is repeated here.

The loading diagram is sketched in Fig. 3.2., whereas Fig. 3.3. shows the actual test rig.

All the electrical measurements were registered automatically on a Solartron, placed to the left in Fig. 3.3. In addition to the time, each scan covered 20 channels, viz.:

- Voltage of the Wheatstone's bridge.
- Load at start of the scan.
- Eight stirrup strain readings (Two opposite each other in the middle of four stirrups placed as shown in Fig.3.2).

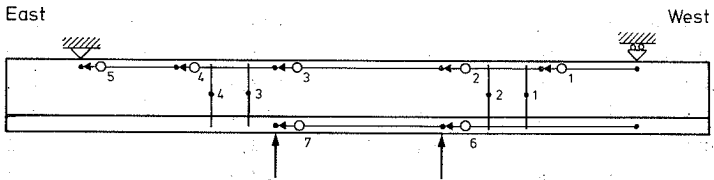


Fig. 3.2 Loading diagram and position of gauge stirrups and dial gauges.

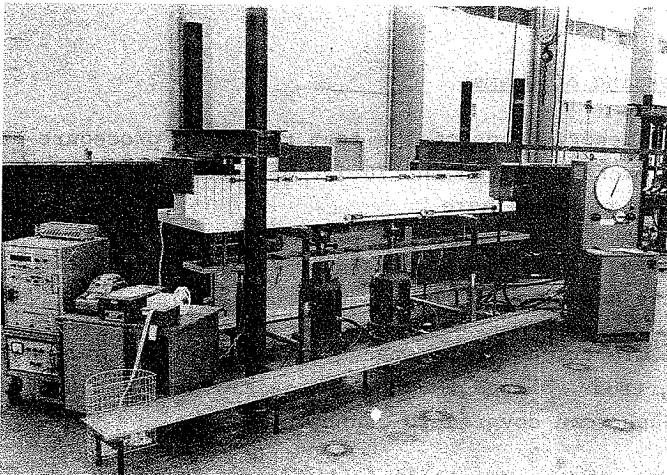


Fig. 3.3 Overall view of beam test rig.

- Nine deflection readings (electric resistance transducers at 300 mm intervals).
- Load at the end of the scan.

Longitudinal strain measurements were taken by means of 7 dial gauges on each side of the beam. The position of the gauges is sketched in Fig. 3.2. The dial gauge readings were recorded visually and the values were later punched onto cards.

A zero measurement was taken with the beam resting on the jacks. The beam was then loaded in steps of 20 kN (per jack), apart from the first steps of 30 kN. Up to about 120 kN, the load was applied for 5 minutes, including 1 minute for the actual loading. The dial gauges were then read and at least 2 scans were taken with a total duration of 2 minutes. At loads of 120 kN or more, the load was applied for 10 minutes before measuring.

The shear cracking load, the load at which the shear cracks extend into the flange and the ultimate load were noted. On the white-washed beam, the cracks were traced with ink and photographed at load intervals of 40 to 60 kN, starting at the cracking load. After failure, the dial gauges and the deflection transducers were removed and an additional photograph was taken.

When one of the shear spans had failed, the corresponding hydraulic jack was closed down and loading proceeded until failure of the other shear span. The shear force in the span is then  $195/300 P$ ,  $P$  being the load on the jack. Therefore, the load steps are increased by a factor of  $300/195 = 1.54$ . The load was raised at intervals of seven minutes. With this second test, only the ultimate load was recorded. In some cases, a second shear failure was not achieved because the beam failed in the same shear span as before.

After completion of the test, close-up photographs were taken of the failure(s) on the opposite sides of the beam where the cracks had not been traced.

#### 4. TEST ANALYSIS

##### 4.1. Computer Programs

Data from the beam was analyzed by the computer program PLOT which was written in FORTRAN and run on the IBM 370/165 computer facilities of NEUCC at the Technical University of Denmark.

Fig. 4.1. shows the structure of the computer program. Analysis is carried out in eight sub-routines, the operation of which is described in [76.1].

The program FLEX calculates the flexural capacity of the beams, based upon the strength of concrete and longitudinal reinforcement, found in Chapter 3. The analysis is explained in [76.1], sec. 2.3. Results are given in Table 4.1.

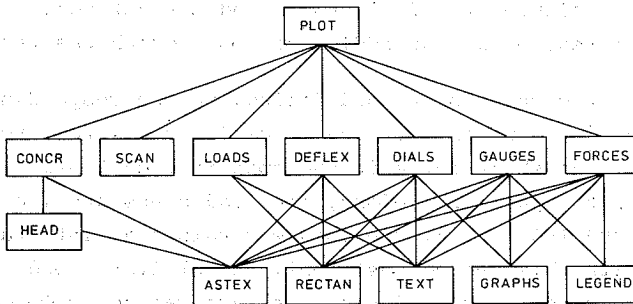


Fig. 4.1 Structure of computer program for analysis of data from beam tests.

Beam no.		$S_y$ (MPa)	$\sigma_c$ (MPa)	$P_F$ (kN)	$V_{cr}$ (kN)	$V_D$ (kN)	Failure mode
V6002	W	0.86	35.7	393	90	245	SW
	E	0.86				253	
V6004	W	1.38	36.4	393	90	306	SW
	E	1.38				347	
U6002	W	0.43	19.5	374	80	194	SW
	E	0.86				200	
U6004	W	0.86	21.1	374	90	224	SW
	E	0.86				237	
U6007	W	1.38	14.7	358	90	204	SW
	E	1.38				218	
U6010	W	1.88	16.5	366	90	265	SE
	E	1.88				260	
U6017	W	2.51	20.1	375	90	306	SW
	E	3.14				326	
U6025	W	4.32	20.2	375	120	365	FT
	E	5.11					
U6007c	W	1.47	18.3	371	90	245	SE
	E	1.47				245	
U6010c	W	2.02	19.3	373	90	286	SE
	E	2.02					
U6013c	W	2.02	12.4	314	90	224	SW
	E	2.02				204	
U6017c	W	3.32	18.3	371	110	306	SE
	E	3.32				265	
U6023c	W	3.94	17.2	368	90	275	SW
	E	3.94				275	
U6029c	W	4.84	20.0	375	60	347	SE
	E	4.84				306	
U6044c	W	8.70	15.0	360	60	265	SW
	E	8.70				265	
U6007h	W	1.47	15.5	362	90	235	SW
	E	1.47				242	
U6010h	W	2.02	17.9	370	90	245	SE
	E	2.02					
U6017h	W	3.34	20.3	376	90	296	SE
	E	3.34				282	
U4213m	W	2.81	14.2	366	90	265	SE
	E	2.84				255	
U4222m	W	5.07	15.8	401	120	357	SE
	E	5.08				316	
U4230m	W	6.38	16.8	423	-	337	SE
	E	6.38				306	
U4244m	W	8.70	16.5	417	90	347	SE
	E	8.70				347	
X6005	W	0.92	7.3	182	60	133	SW
	E	0.92				143	
X6018	W	1.84	9.4	261	60	235	SE
	E	1.84				219	
X9032	W	2.94	8.5	260	60	184	SW
	E	3.09				204	
X9043	W	4.07	8.2	253	60	184	SW
	E	4.06				201	
B6009	W	0.87	10.7	340	90	286	SE
	E	0.80				245	
B9018	W	1.87	10.1	280	90	286	FT
	E	1.91					
B9025	W	3.16	11.1	299	90	286	FT
	E	3.14					
B9025a	W	2.67	12.3	437	90	439	SE
	E	2.91				408 *	
B9029	W	2.86	9.7	463	90	388	SW
	E	2.63				428 **	
B9040	W	4.17	8.6	439	120	388	SW
	E	4.17				449 ***	
U5617i	W	2.92	17.9	403	60	336	SW
	E	2.69				326	
U5604p	W	1.05	24.1	415	-	255	SE
	E	1.05				235	
R4251	W	4.58	9.6	436	90	346	SW
	E	4.46				356	
R5651	W	4.44	9.3	240	140	275	SW
	E	4.25				255	
S9013	W	1.36	9.4	257	80	184	SW
	E	1.34				184	
S9039	W	3.75	11.5	318	120	316	FT
	E	3.75					
S9040	W	3.69	7.8	312	120	265	SE
	E	3.69					
S9050	W	4.36	8.2	312	150	306	SE
	E	4.36					

\* main reinforcement curtailed  
 \*\* second test flexural failure  
 \*\*\* second test shear failure in flexural zone

Table 4.1 Strength properties of test beams.



Finally, the program EXP compares the experimentally obtained ultimate loads with the predictions of the theory (cf. sec. 1.1.). The program calculated the best value of the web effectiveness  $v$  by minimizing the sum of squares of the normal distances of the experimental points  $(\psi, \tau/\sigma_c)$  from the theoretical curve, equation (2). The output includes the coefficient of variation based upon  $N - 1$  degrees of freedom,  $N$  being the number of points. The results are given in sec. 4.7.

The actual programs are listed in [76.1], Appendix A. The entire output is collected in Appendix A of this report. A general description of the results is given in [76.1] and the following sections.

#### 4.2. General Behaviour

The structural properties of the 40 statically tested beams are listed in Table 4.1. (The fatigue tests are treated in sec. 6.) The table contains the material strengths  $\sigma_c$  and  $s_y$ , (cf. Sec.3.2 and Sec.3.3, respectively), the expected flexural failure load  $V_F$ , the observed ultimate load  $V_u$  and the type of failure. The latter is designated as follows: SE: shear failure of eastern span, SW: shear failure of western span, FT: flexural tension failure, FC: flexural compression failure.

The shear cracking load  $V_{cr}$  is defined as the load step at which the first visible web crack appeared.

The ultimate load is defined as the maximum load recorded on the manometer, i.e. the load at which the pressostate is unable to keep up with the deformations.

At about 75% of the ultimate load, the shear cracks extended into the flange. At this stage, the deformations become considerable and the beam assumes a characteristic S - shape with reversal of curvature at the supports. Immediately prior to failure, this leads to the formation of tensile cracks in the flanges near the supports.

Even quite close to the ultimate load, it remained an open question as to which shear zone was going to fail first. Neither the location of the first visible crack, nor the extension of the cracks into the flange could be taken as a guide. The only infallible indication was the appearance of the tensile flange cracks, as mentioned above.

In the cases where two shear failures were obtained by the procedure described in Sec.3.5, the second failure load was always equal to, or slightly higher than the first. This indicates that the second failure load may be used with confidence although the moment distribution in the beam is somewhat different.

It is worth noting that the two failure loads for the same beam may differ as much as 12%, although the strength properties of the two shear spans are supposedly identical. Thus, a theoretical prediction of load carrying capacity must be subject to an unreliability of this order of magnitude.

#### 4.3. Loads, Deflections and Dial Gauge Readings

The complete results of these measurements are given in Appendix A and a general description is given in [76.1].

In Table 4.2., the maximum deflection is given for each beam at a load of 50 - 60% of the ultimate shear load, corresponding to the service load. It can be seen that the deflection at this load only exceeds 10 mm in a few cases.

#### 4.4. Stirrup Strains and Forces

Measurements of stirrup strains and forces are also collected in Appendix A. A general description of these measurements is given in [76.1].

As an example, the stirrup force curves of beam U6007 are shown in Fig. 4.1. At a loading stage of about 90% of the failure load, stirrup No. 1 yields, whilst the other stirrups have not yet reached yielding force. Furthermore, it is seen that the stirrup force remains negligible until shear cracking occurs.

Beam no.	Service load 0.5-0.6 V <sub>u</sub> (kN)	Maximum deflection at service load (mm)
V6002	122	3.8
V6004	159	6.3
U6002	122	5.2
U6004	143	5.9
U6007	121	6.1
U6010	142	6.5
U6017	182	8.5
U6025	183	7.7
U6007c	142	6.6
U6010c	157	7.0
U6013c	122	5.7
U6017c	162	7.0
U6023c	142	6.4
U6029c	162	7.3
U6044c	142	6.0
U6007h	142	6.1
U6010h	142	6.2
U6017h	142	6.2
U4213m	142	5.2
U4222m	159	5.7
U4230m	162	4.9
U4244m	182	6.0
X6009	81	7.6
X9018	120	7.8
X9032	121	9.0
X9043	123	9.3
B6009	152	7.0
B6018	152	8.9
B6025	162	10.0
B6025a	202	9.7
B6029	213	13.6
B6040	214	10.9
U5617i	182	8.2
U5604p	142	5.3
R4251	185	5.5
R5651t	142	7.7
S9013	101	11.8
S9039		
S9040	142	9.3
S9050	152	10.1

Table 4.2 Deflections at service load  
(= 0,5 - 0,6 × ultimate load).

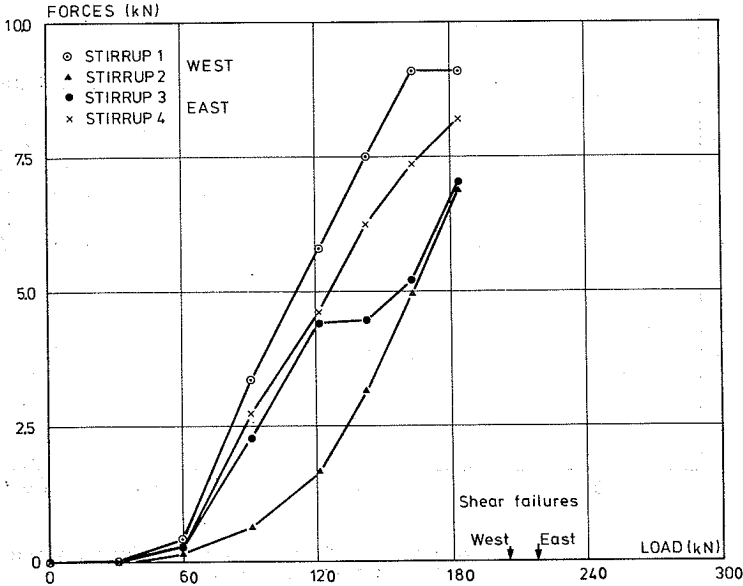


Fig. 4.1 Stirrup force curves for Beam No. U6007.

The outcome of an investigation of stirrup yield for all the test beams is shown in Table 4.3. Corresponding to each beam, the table lists the failure mode (cf. Sec. 4.2) and the results of an examination of each stirrup. The symbols used are explained in the caption to the table. Finally, the beam is classified according to yield of the stirrups.

In Fig. 4.2., the maximum recorded stirrup force from Table 4.3. is plotted against the reinforcement degree  $\psi$ . It can be seen that for  $\psi > 0.2$ , yield of stirrup at failure is not always detected, and for  $\psi > 0.3$ , yield is never detected.

In a few beams, (U6023c, U6029c, X8009 and X9018) the force in the horizontal, lower part of the stirrup was measured. Generally, these measurements did show that this force is only half of the force in the vertical stirrup legs (see Fig.4.3).

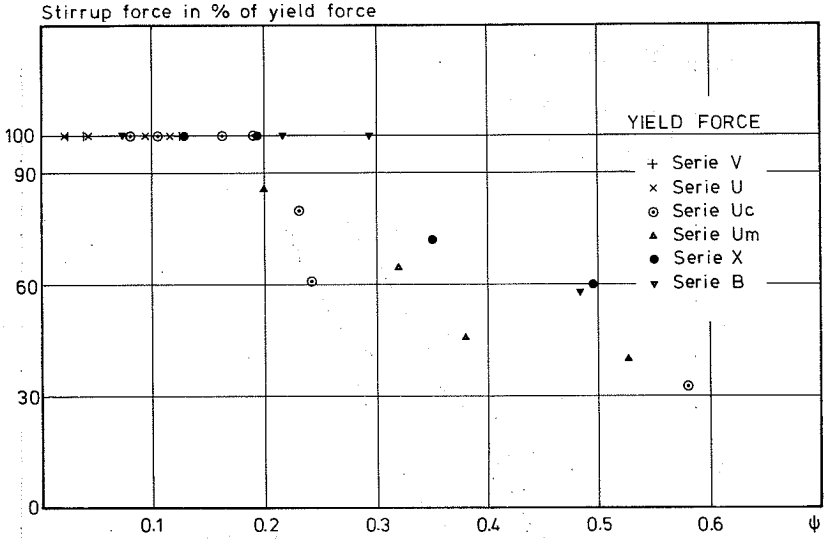


Fig. 4.2 Maximum recorded stirrup force versus the reinforcement degree,  $\psi$ .

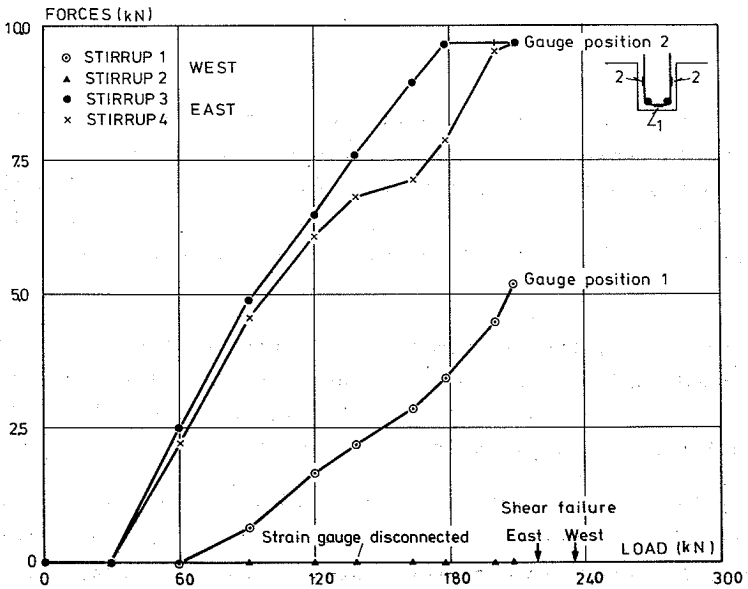


Fig. 4.3 Stirrup force curves for Beam No. X9018

	Failure mode	WEST		EAST		Yield
		Stirrup 1	Stirrup 2	Stirrup 3	Stirrup 4	
V6002	SW	Y	Y	Y	Y	Y
V6004	SW	Y	Y	Y	(Y)	Y
U6002	SW	Y	(Y)	Y	(Y)	Y
U6004	SW	Y	0.92	(Y)	(Y)	Y
U6007	SW	Y	0.98	(Y)	(Y)	Y
U6010	SE	Y	(Y)	(Y)	Y	Y
U6017	SW	Y	0.98	0.89	0.84	Y
U6025	FT	0.77	0.83	0.69	0.61	0
U6007c	SE	Y	Y	(Y)	Y	Y
U6010c	SE	Y	Y	Y	0.47	Y
U6013c	SW	(Y)	Y	0.86	0.90	Y
U6017c	SE	0.65	0.90	0.93	(Y)	(Y)
U6023c	SW	0.80	0.31*	0.42	0.21*	0
U6029c	SE	0.53	0.42	0.30*	0.61	0
U6044c	SW	0.31	0.26	0.24	0.33	0
U6007h	SW	Y	Y	Y	Y	Y
U6010h	SE	0.88	0.88	0.93	0.96	0
U6017h	SE	0.76	0.69	0.64	0.67	0
U4213m	SE	0.81	0.76	0.86	0.80	0
U4222m	SE	0.85	0.70	0.64	0.65	0
U4230m	SE	0.38	0.41	0.36	0.46	0
U4244m	SE	0.47	0.48	0.30	0.40	0
X6009	SW	(Y)	Y	Y	0.93*	Y
X9018	SE	0.78*	÷	Y	Y	Y
X9032	SW	0.56	0.72	0.61	0.72	0
X9043	SW	0.49	0.60	0.58	0.58	0
B6009	SE	(Y)	(Y)	(Y)	(Y)	(Y)
B9018	FT	0.66	0.55	0.53	0.57	0
B9025	FT	0.32	0.38	0.14	0.36	0
B9025a	SE	(Y)	(Y)	0.67	0.78	(Y)
B9029	SW	(Y)	0.70	÷	Y	Y
B9040	SW	0.40	0.46	0.58	0.58	0
U5617i	SW	(Y)	Y	(Y)	Y	Y
U5604p	SE	0.79	0.46	÷	÷	0
R4251	SW	Y	Y	0.88	0.33	Y
R5651	SW	÷	0.91	0.67	0.85	0
S9013	SW	0.93	0.93	(Y)	0.50	(Y)
S9039	FT					
S9040	SE	0.92	÷	0.92	0.91	0
S9050	SE	0.89	0.97	0.96	0.85	0

Y : Yielding detected at last loading stage before failure  
(Y): Extrapolation indicate yielding at failure load  
÷ : Strain gauges disconnected or inoperable  
\* : Strain gauges at the horizontal part of stirrup  
0,0.xx : No yielding at failure load, ratio between stirrup stress at failure load and yield stress

Table 4.3 Recording of stirrup yield

#### 4.5 Cracking and Crack Width

Photographs of the crack development of each beam are collected in Appendix A, together with pictures of both the shear spans after failure and of the reinforcement.

Measurements of the crack widths were only taken for the series B and series S. For series B, the maximum crack width at the service load (50 - 60% of the failure load), was not greater than 0.2 mm. For series S, the maximum crack width was less than 0.1 mm.

#### 4.6 Ultimate Loads and Web Effectiveness Parameter

##### 4.6.1 Results of All Series

As described in Sec. 4.2, the beam tests yielded 67 shear failures plus 4 flexural failures. The tests were grouped in 11 series: V (4 failures), U (10 + 1 failures), U<sub>c</sub> (13 failures), U<sub>h</sub> (5 failures), U<sub>m</sub> (8 failures), X (4 failures), X<sub>d</sub> (4 failures), B (4 + 2 failures), B<sub>d</sub> (3 failures), SPB (8 failures) and S (4 + 1 failures).

All test results are summarized in Table 4.4. The table lists the non-dimensional parameters,  $\psi$ ,  $\tau/\sigma_c$  and  $\nu$ . According to the theory, the point  $(\psi, \tau/\sigma_c)$  should either lie on a circle with diameter  $\nu$ , or on its horizontal tangent. The value  $\nu$ , given in Table 4.4 for each shear test, is the diameter of the circle on which the particular point  $(\psi, \tau/\sigma_c)$  is located. For points with  $\psi > \tau/\sigma_c$  we have put  $\nu = 2 \tau/\sigma_c$ , assuming that the point lies on the tangent.

In Fig.4.4, all the test results (except the results of the special beams of series U<sub>h</sub> and series SPB) are plotted. By means of program EXP, described in Sec.4.1, the theoretical curve giving closest fit is drawn. The corresponding  $\nu$ -value is 0.70 and the coefficient of variation 9.6%. Fig.4.5 shows the same plot, but with the results of series T, T<sub>d</sub> and T<sub>m</sub>, reported in [76.1] included. This changes the best  $\nu$ -value and the coefficient of variation slightly to 0.73% and 9.0%, respectively.

Beam no.		$\psi$ (%)	$\tau/\sigma_c$ (%)	$v$ (%)	Beam no.		$\psi$ (%)	$\tau/\sigma_c$ (%)	$v$ (%)
V6002	W	2.4	11.5	57.4	U4230m	W	38.0	34.0	68.0
	E	2.4	11.9	61.1		E	38.0	30.9	61.7
V6004	W	3.8	14.1	56.3	U4244m	W	52.7	35.6	71.3
	E	3.8	16.0	71.3		E	52.7	35.6	71.3
U6002	W	2.2	16.7	128.6	X6009	W	12.6	29.1	79.8
	E	2.2	17.2	136.5		E	12.6	31.3	90.3
U6004	W	4.1	17.8	81.9	X6018	W	19.6	40.6	103.7
	E	4.1	18.8	91.2		E	19.6	37.8	92.7
U6007	W	9.4	23.3	67.1	X9032	W	34.9	35.6	71.2
	E	9.4	24.9	75.3		E	36.4	39.5	79.2
U6010	W	11.4	26.9	75.1	X9043	W	49.6	36.9	73.8
	E	11.4	26.4	72.7		E	49.5	40.3	80.6
U6017	W	12.5	25.5	64.7	B6009	W	8.1	22.8	71.9
	E	15.6	27.2	63.0		E	7.5	19.5	58.3
U6025		21.4	flex.fail.		B9018		18.5	flex.fail.	
U6007c	W	8.0	22.5	70.8	B9025		28.7	flex.fail.	
	E	8.0	22.5	70.8					
U6010c	W	10.5	24.9	69.5	B9025a	W	21.7	30.4	64.3
	E					E			
U6013c	W	16.3	30.3	72.7	B9029	W	29.5	34.1	68.8
	E	16.3	27.6	63.1		E	27.1	37.6	79.2
U6017c	W	18.1	28.1	61.5	B9040	W	48.5	38.4	76.8
	E	18.1	24.3	50.7		E	48.5	44.5	80.9
U6023c	W	22.9	26.8	54.3	U5617i	W	16.3	30.4	72.8
	E	22.9	26.8	54.3		E	15.0	30.4	76.3
U6029c	W	24.2	29.1	59.2	U5604p	W	4.3	17.6	76.4
	E	24.2	25.7	51.4		E	4.3	16.3	65.5
U6044c	W	58.0	29.6	59.3	R4251	W	47.7	57.4	116.1
	E	58.0	29.6	59.3		E	46.5	59.0	121.5
U6007h	W	9.5	25.4	77.7	R5661t	W	47.7	47.1	94.2
	E	9.5	26.2	81.8		E	45.7	43.7	87.3
U6010h	W				S9013	W	14.5	31.6	83.4
	E	11.3	23.0	58.0		E	14.5	31.6	84.2
U6017h	W	16.5	24.5	52.8	S9039			flex.fail.	
	E	16.5	23.3	49.5					
U4213m	W	19.8	31.6	70.3	S9040	W	47.3	54.8	110.8
	E	20.0	30.4	66.3		E			
U4222m	W	32.1	38.3	77.8	S9050	W	53.2	60.2	121.3
	E	32.2	33.9	67.9		E			

Table 4.4 Test results from all static tests.



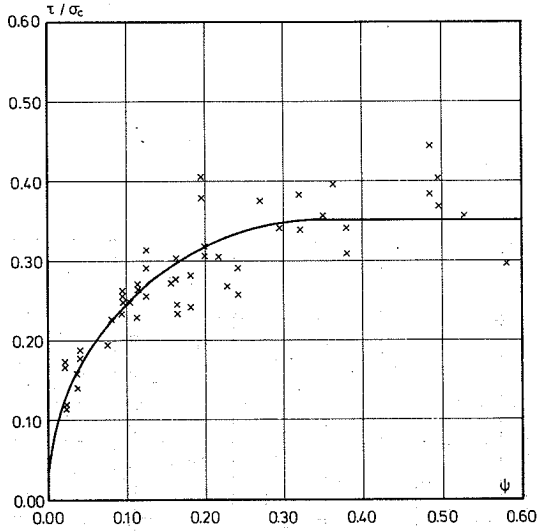


Fig.4.4 Results of all shear tests,  $\nu = 0.70$ , coefficient of variation 9.6%

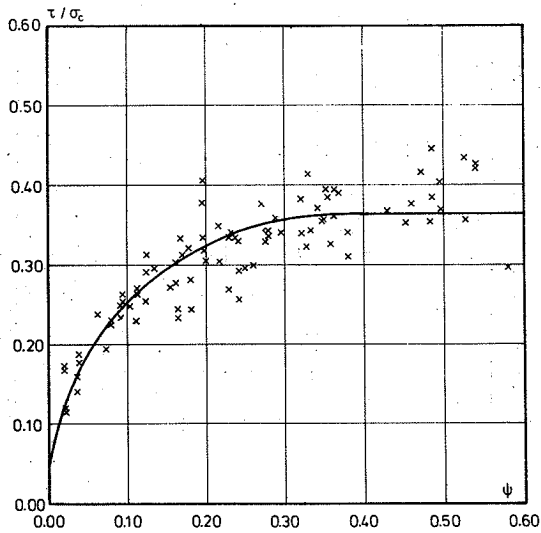


Fig.4.5 Results of all shear tests with series T, included,  $\nu = 0.73$ , coefficient of variation 9.0%

#### 4.6.2. Results of the Individual Series

In Figs. 4.6 - 4.16, the results of the individual series are plotted and the theoretical curve giving closest fit is drawn. The corresponding  $\nu$  - values and coefficients of variation are listed in Table 4.5.

With the aid of the test series, the dependence of  $\nu$  on the following parameters was investigated to a reasonable degree of thoroughness:

- Diameter of tensile reinforcement.
- Concrete cover.
- Stirrup layout.
- Width of web.
- Concrete strength.
- Stirrup inclination.

The results are briefly discussed below:

Influence of the tensile reinforcement diameter,  $d$ , is examined by the series U ( $d = 25$  mm) and Um ( $d = 35$  mm) with a planned concrete strength of 20 MPa and by the series T ( $d = 16$  mm) and X ( $d = 12$  mm) with a planned concrete strength of 10 MPa.

Because of uncontrolled fluctuations in the concrete strength, (the average values of the series varying from 8 MPa to 19 MPa), the results concerning this point were not quite clear. However, the variations in the  $\nu$  - values are most likely due to the variation in concrete strength. A tentative conclusion is then that there is no significant dependence on the diameter.

Influence of the concrete cover was investigated through series T and Tm and series U and Uc. The results indicated a decrease in  $\nu$  - value with increasing concrete cover.

Dependence of  $\nu$  on the number of bars supported by stirrup bend was studied by series (T, Td), (X, Xd) and (B, Bd) respective

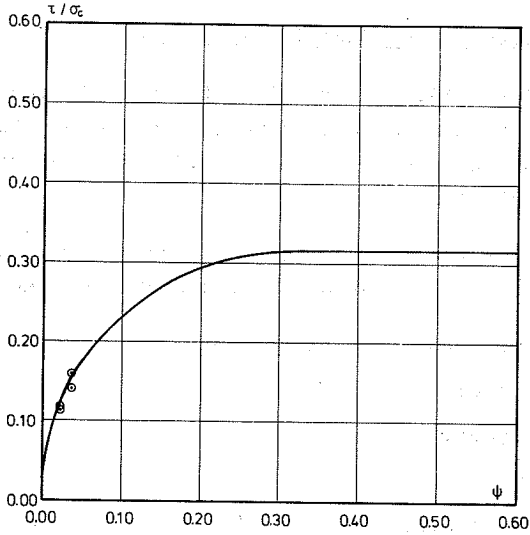


Fig. 4.6 Results of series V ( $\nu = 0.63$ )

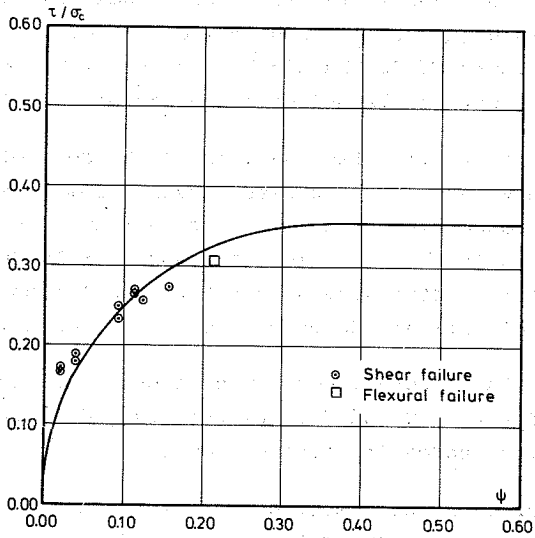


Fig. 4.7 Results of series U ( $\nu = 0.73$ )

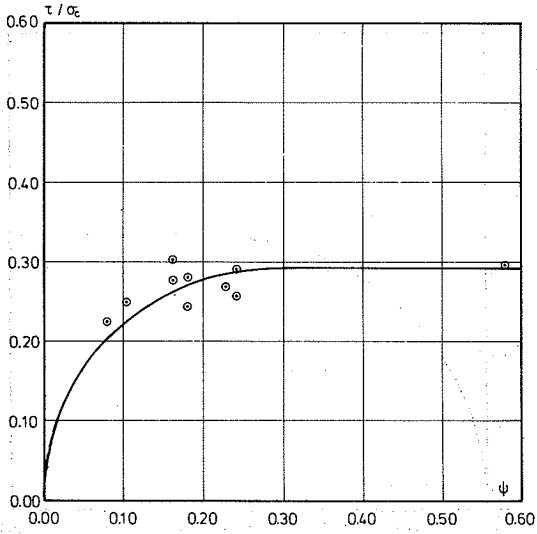


Fig. 4.8 Results of series Uc ( $\nu = 0.58$ )

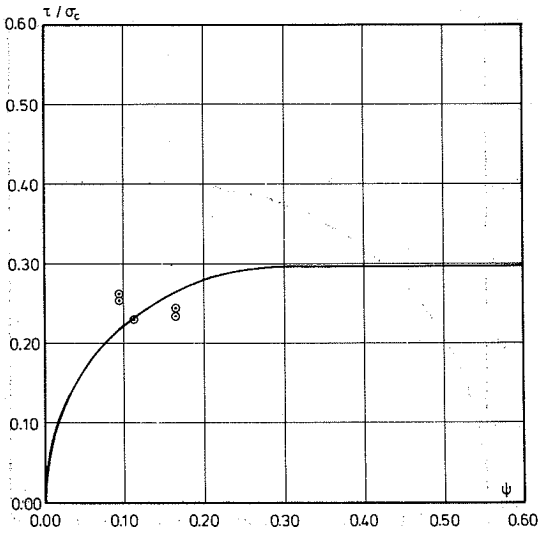


Fig. 4.9 Results of series Uh ( $\nu = 0.59$ )

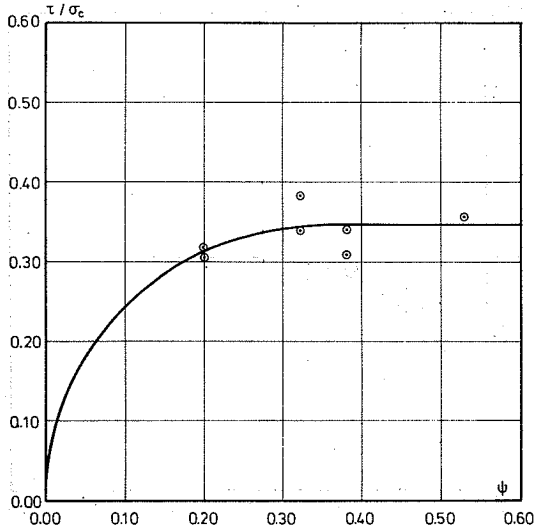


Fig. 4.10 Results of series  $U_m$  ( $\nu = 0.69$ )

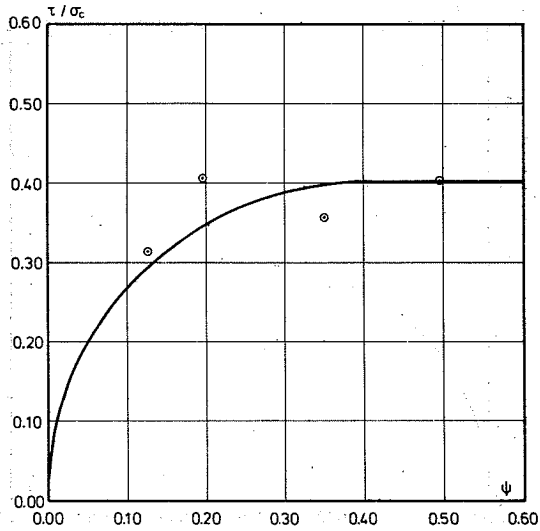


Fig. 4.11 Results of series  $X$  ( $\nu = 0.80$ )

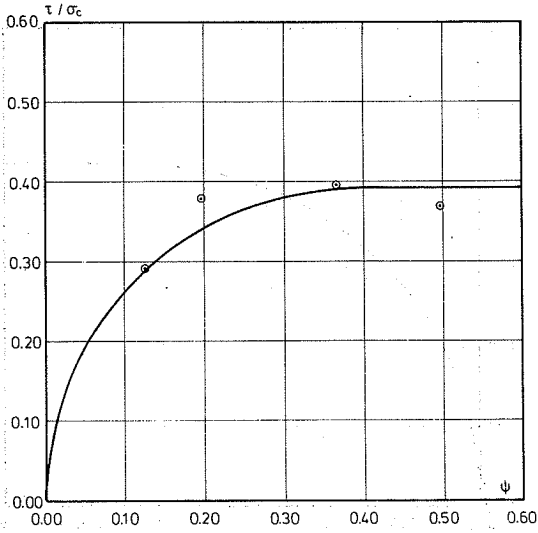


Fig. 4.12 Results of series Xd ( $\nu = 0.78$ )

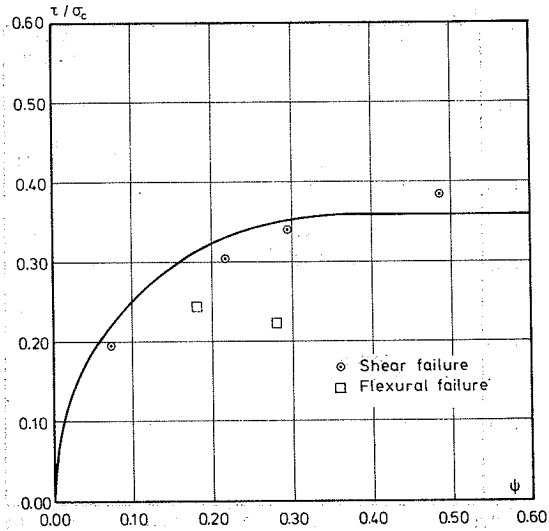


Fig. 4.13 Results of series B ( $\nu = 0.72$ )

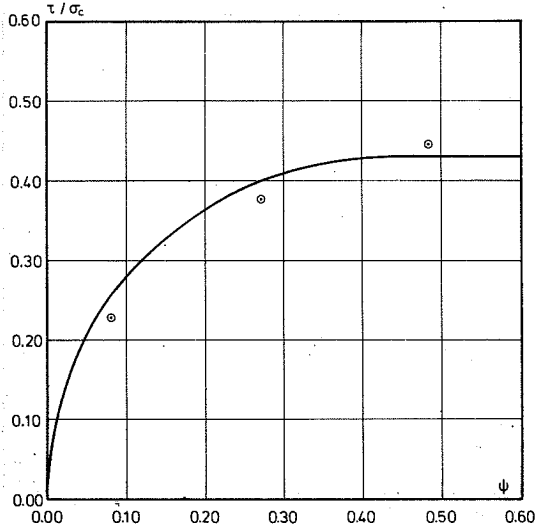


Fig. 4.14 Results of series Bd ( $\nu = 0.86$ )

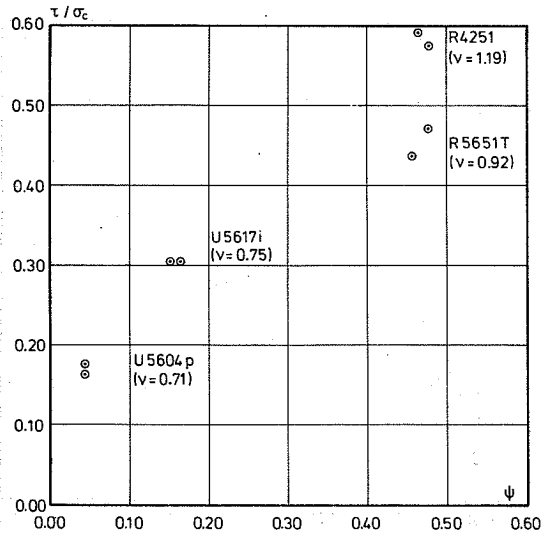


Fig. 4.15 Results of series SPB

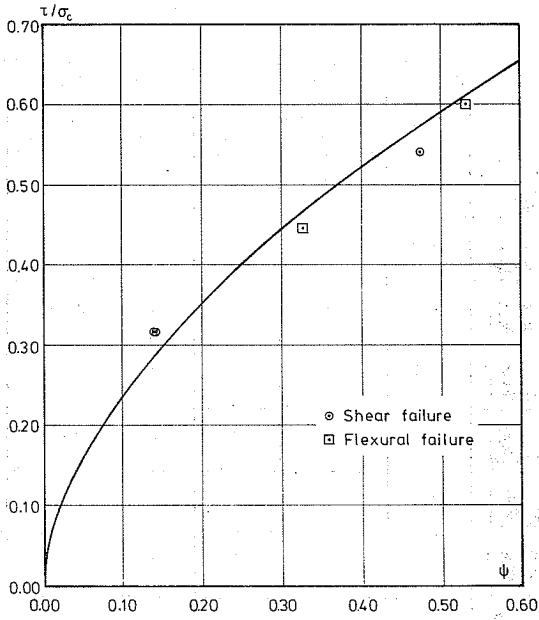


Fig. 4.16 Results of series S ( $\nu = 0.72$ )



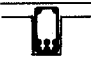




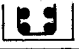


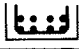


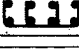
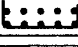
Series	Stirrup arrangement	Average concrete strength $\sigma_c$ MPa	Diameter of tensile reinforcement d (mm)	Concrete cover e (mm)	Number of shear tests	Effectiveness parameter	
						Average value	Coefficient of variation %
T		11.1	16	24	36	0.74	7.4
Tm		11.2	16	12	4	0.79	5.4
Td		10.4	16	24	4	0.69	10.6
V		36.0	25	24	4	0.63	1.2
U		18.7	25	24	10	0.70	3.6
Uc		17.2	25	50	13	0.58	7.0
Uh		17.9	25	50	5	0.59	9.6
Um		15.8	35	12	8	0.69	6.2
X		8.4	12	24	4	0.80	10.0
Xd		8.4	12	24	4	0.78	6.2
B		10.4	16	24	4	0.72	6.4
Bd		10.4	16	24	3	0.86	5.0
S		9.2	12	24	3	0.72	

Table 4.5 Average  $\nu$  - values of test series

For the series with a web width of 200 mm, there is no significant difference in  $v$  - values. However, series B and Bd, with a width of 380 mm, show a clear increase in  $v$  when 4 bars are supported instead of 2.

Efficiency of hairpin stirrups was investigated in the series Uh (hairpin stirrups) and Uc (ordinary stirrups). No difference in the  $v$  - values was detected.

The dependence of  $v$  on the beam width was examined by the series T, Td ( $b = 200$  mm) and B, Bd ( $b = 380$  mm). When the corner bars only are supported by the stirrup bends, there is no difference in the  $v$  - values. When all bars are stirrup supported, the increase in  $v$  - values for the wide beams is significant.

Plans were made to obtain an indication of the influence of concrete strength by comparing the results of series V ( $\sigma_c = 360$  MPa) and series U ( $\sigma_c = 190$  MPa). The results suggest that  $v$  decreases with increasing concrete strength. If the variation in diameter of the main reinforcement is neglected, the results of the series T, Um and X can also be included. The outcome (see Fig. 4.17) shows a dependence of  $v$  on the concrete strength which is excellently described by the linear relationship

$$v = 0.8 - \frac{\sigma_c}{200} \quad (\sigma_c \text{ in MPa}) \quad (4.1)$$

Because of two flexural failures in the series with inclined stirrups, (series S), a well-defined value for the magnitude of  $v$  was not obtained, (see Fig. 4.16), but the test results at least do not contradict that  $v$  on an average has the same magnitude as for beams with vertical stirrups.

#### 4.6.3. Results of Tests with Special Beams

Results of the pilot tests with special beams, series SPB (see Sec.2.3.), are shown in Fig. 4.15. and they suggest the following rather tentative conclusions:

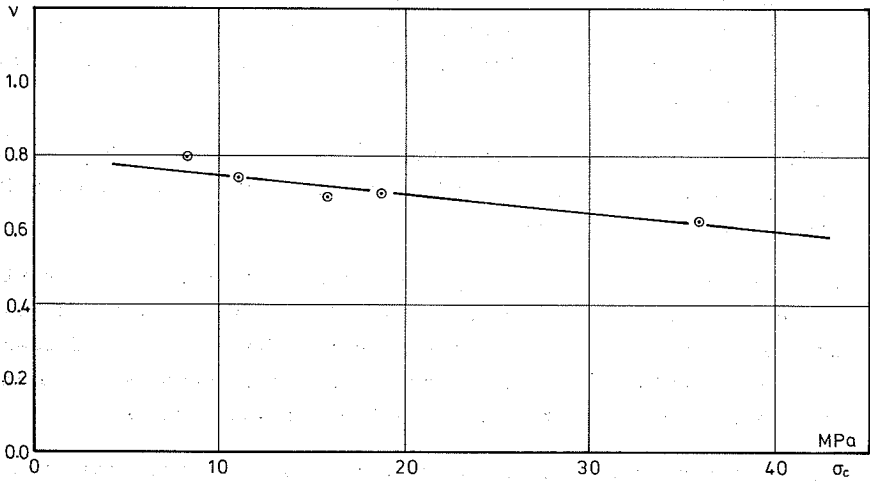


Fig. 4.17 The  $v$  - dependence of the concrete strength

- U5617i indicates no reducing effect when placing the tensile reinforcement away from the stirrup bends.
- R5651t suggests an increasing  $v$  - value with decreasing stirrup spacing.
- R4251 shows a considerable increase in  $v$ , - even beyond unity, if the tensile reinforcement bars are replaced by a steel plate with the stirrups welded to the plate.
- U5604p gave the result that  $2 \cdot 10^6$  pulsations at service load do not reduce the  $v$  - value.

## 5. DISCUSSION AND CONCLUSIONS

### 5.1 Failure Mechanisms

The behaviour of all the beams follows the pattern stated in Sec. 1.1 of [76.1] quite well.

Discussion of the failures of the beams in series T, given in Sec. 5.1 of [76.1], is generally valid for beam failures in the series described in this report.

In Fig.5.1, a typical failure for each series is shown. There was no remarkable difference in the failure pictures. The most outstanding failures were those of series Uc and Uh, i.e. the series with the large concrete cover. These series showed a clear tendency of the concrete cover to spall immediately prior to failure. The effect is clearly seen in Fig.5.2.

Three beams were cut through in a normal section of the failed shear zone to study cracking inside the web. The three beams, U6017, U6017c and U6017h, had a different concrete cover or stirrup arrangement. Cross sections and the crack pattern are shown in Fig. 5.3. These crack patterns supply no information about differences of the failure mechanisms of the beams, but they confirm the result of the cut-through, reported in [76.1]. The observed crack pattern on the faces of the beam did not penetrate the web.

In connection with the cutting, a beam in series T, - T6029, - was injected with epoxy and then cut up in the vertical plane of symmetry of the beam, leaving the whole central part of the shear zone ready for inspection of crack patterns. However, the epoxy injection, intended to establish a tracing of the inside cracking, did not succeed, only the concrete cover was penetrated. Because of this, the crack pattern on the cut faces became too vague to supply further information about the mechanism of shear failure.

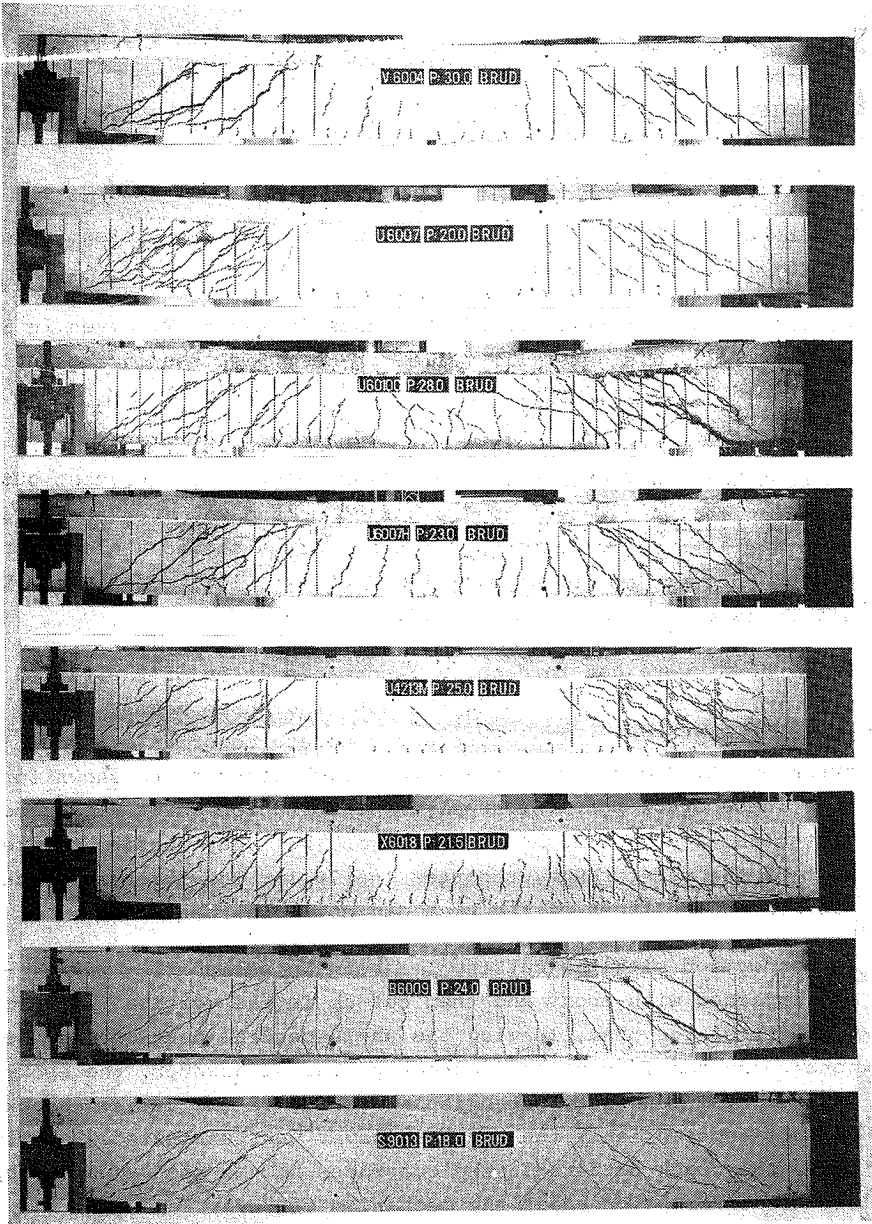


Fig.5.1 Failure pictures for the beams V6004, U6007, U6010c, U6007h, U4213m, X6018, B6009 and S9013. The failure loads are here given in Mp

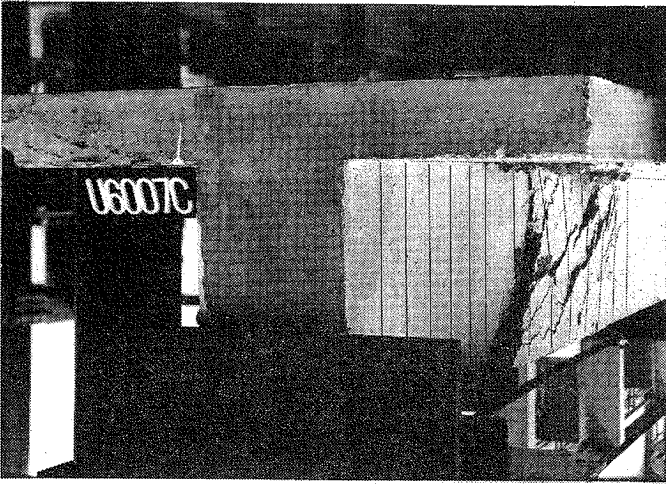


Fig. 5.2 Shear failure of Beam No. U6007c.

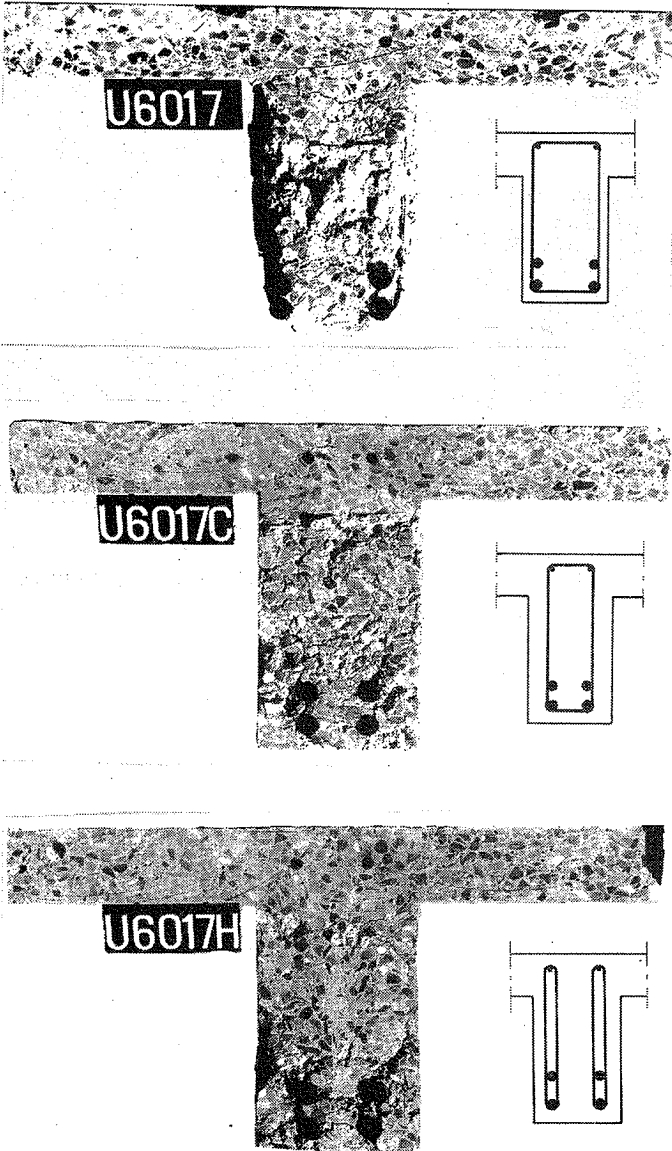


Fig. 5.3 Normal sections of the beams U6017, U6017c and U6017h

## 5.2 Strong Shear Reinforcement

In the test series Uc, Um, X and B, test beams with a very strong shear reinforcement are included. These tests support the results of [76.1], i.e., that the load-carrying capacity is independent of the amount of shear reinforcement, provided that the latter is of sufficient magnitude.

The reason for this is that the concrete of the web fails before the stirrups yield. Thus, the degree of shear reinforcement,  $\psi = \psi_1$  necessary for the occurrence of this situation may be deduced from the observations of stirrup yield. Such observations were illustrated in Fig. 4.3. and they suggest that  $\psi_1$  lies in the interval  $0.2 < \psi_1 < 0.3$ .

This result is not in accordance with the theory from which we would expect yielding of stirrups in the interval  $0.3 < \psi_1 < 0.4$ . A possible explanation of this discrepancy is that even if yield is not detected in the stirrups supplied with gauges, it could have started in other stirrups.

## 5.3. Calculation of Effectiveness Parameters

One of the main purposes of the test program was to establish a model for the calculation of  $v$  when the section geometry and strength parameters were given. In the following, different models are suggested, and their agreement with the experimental  $v$  - values is discussed.

One model was based on the hypothesis that  $v$  is less than unity because of the stress concentration above the main reinforcement bars. The force from the stirrups is transferred to the main reinforcement bars which in turn are supported by the web concrete. Thus, the web compression is concentrated at the longitudinal bars and this concentration gives rise to failure before the average stress in the web reaches the uniaxial compressive concrete strength. This means that the effective concrete strength,  $\sigma^*_c$ , can be calculated as:

$$\sigma^*_c = \frac{nd\beta\sigma_c}{b} \quad (5.1)$$



and then

$$v = \frac{nd\beta}{b} \quad (5.2)$$

Here,  $d$  is the diameter of the longitudinal bars  $b$  is the width of the beam web,  $n$  is the number of bars supported by stirrup bends,  $\sigma_c$  is the cylinder strength and  $\beta\sigma_c$  is the maximum compression on a longitudinal bar.

It is assumed here that only the bars supported by stirrup bends are capable of transferring the force from the stirrup to the concrete. This assumption is based on tests by Malling [72.1] and Leonhardt & Walther [63.11].

On the basis of the same tests,  $\beta$  was initially chosen to  $\beta = 3.0$ , (Malling and Leonhardt tests give the values 3.2 and 2.8. respectively).

In accordance with this model,  $v$  is proportional to  $d$  and  $n$  and inversely proportional to  $b$ . As seen by the analysis of the results in sec. 4.6.2., these trends are in no way supported by the experimental results, according to which  $v$  is almost independent of  $d$ ,  $n$  and  $b$ . In Table 5.1., quantitative results of the model are compared with the experimental values.

A reason for the bad correspondance could be that  $\beta$  actually is not a constant. If the web failure is assumed to follow a logarithmic spiral, (see Fig. 5.7.),  $\beta$  is found to be an increasing function of  $e/d$  (concrete cover/diameter of bars). The series X and Um with the extreme value of  $e/d$ , 2 and 0.34 respectively were carried out to test this assumption.

Generally speaking, this model produces better results when  $\beta$  is calculated in this way, but the results are still not satisfactory. Firstly, the model now predicts increasing  $v$ -values with increasing concrete cover, whilst the experiments show the opposite tendency and, secondly, the model still claims  $v$  to be inversely proportional to the width.

Even if the result could be further improved by using other values

Series	$v = \frac{n\beta d}{b}$	$\bar{v}$
T	0.48	0.74
Tm	0.48	0.79
Td	0.72	0.69
V	0.75	0.63
U	0.75	0.70
Uc	0.75	0.58
Um	1.05	0.69
X	0.36	0.80
Xd	0.72	0.78
B	0.25	0.72
Bd	0.50	0.86

Table 5.1 Average  $v$  - values compared with the expression  $v = n\beta d/b$

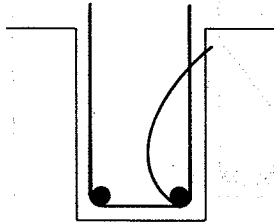


Fig. 5.4 Web failure

of  $\alpha$  and maybe  $n$ , (the total number of bars in the bottom layer), this model could never explain the observed dependency of  $v$  on the width, and therefore the model must be rejected.

These results lead to the suggestion that the failure is not a local phenomenon at the longitudinal bars, but involves the entire web. In other words, irrespective of the stirrup arrangement, the web strength is governed by the strength of the concrete body enclosed by the stirrup.

Adopting this point of view, the theoretical determination of the web strength is reduced to a plane problem. We consider a section parallel to the inclined concrete struts and idealize the action of the stirrups as a uniformly distributed strip load,  $\sigma_f$ , over the stirrup width,  $b_s$ , (see Fig.5.5).

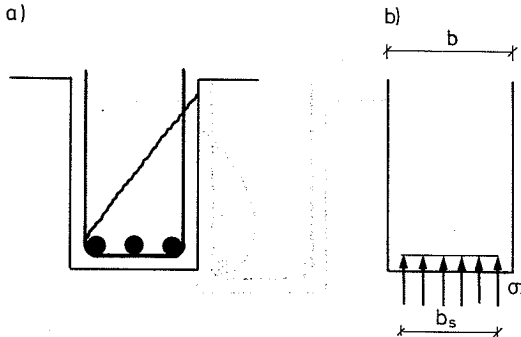


Fig. 5.5 Web failure  
a. Possible failure mechanisms (normal section)  
b. Web crushing idealized as a strip load on a prismatic concrete body (inclined section)

Data concerning concentrated loads on concrete prisms has been compiled by Jensen [74.1], who concludes that the ultimate stress on the loaded area can be calculated by the formula

$$\frac{\sigma_f}{\sigma_c} = 0.2 + 0.8 \sqrt{\frac{b_s}{b}} \quad (5.3)$$

where  $b$  is the part of the supported area (width) which is symmetrical with respect to the centre line of  $b_s$ . Hence the web effectiveness parameter is determined by

$$v = \frac{b_s \sigma_f}{b \sigma_c} = 0.2 \frac{b_s}{b} + 0.8 \sqrt{\frac{b_s}{b}} \quad (5.4)$$

where  $b_s/b = 1 - (2e/b)$ ,  $e$  being the concrete cover. To obtain a simple formula, the square root is replaced by the first term of a series expression, i.e.  $b_s/b = 1 - (e/b)$ , (for  $e/b < 0.125$ , the error does not exceed 1%). Thus we obtain

$$v = 1.0 - 1.2 \frac{e}{b} \quad e/b < 0.125 \quad (5.5)$$

as an approximate expression for the dependence of  $v$  on the concrete cover.

According to this model,  $v$  decreases with increasing concrete cover and increases with increasing beam width. From sec. 4.3.2., it can be seen that these predictions are qualitatively in accordance with the experimental results.

In Fig. 5.6., the model is compared with the experimentally determined  $v$  - values of the individual series. The plot includes the point corresponding to series  $U_c$ , although it falls outside the range of equation (5.5). ( $e/b = 0.25$ ). The model clearly overestimates the  $v$  - values. However, a reasonable agreement can be obtained if  $v$  is modified to

$$v = 0.84 (1.0 - 1.2 \frac{e}{b}) = (0.84 - 1.0 \frac{e}{b}) \quad (5.6)$$

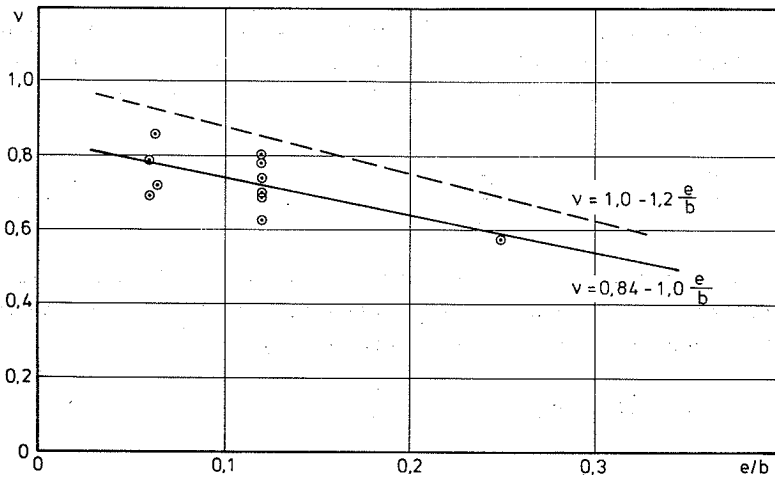


Fig. 5.6 The average  $\nu$  - values compared to empirical model

where the constant factor is determined by requiring the mean of the calculated best  $\nu$  - values equal to the mean of the experimental values. The standard deviation is calculated as 0.062.

Results from application of the plasticity theory to punching shear and shear in beams without shear reinforcement have shown a marked tendency of  $\nu$  to decrease with increasing concrete strength. In both cases, the variation of  $\nu$  has been described by an inverse square root dependence  $\nu = k_1/\sqrt{\sigma_c}$  where  $k_1$  is a constant. However, for shear reinforced beams, this model underestimates the  $\nu$  - values for the high concrete strengths ( $\sigma_c > 20$  MPa).

For the series where, besides the concrete strength, only the diameter of the reinforcement bars is varied, we found an excellent agreement with the linear relationship (see Sec. 4.6.2.)

$$v = 0.8 - \frac{\sigma_c}{200} \quad (\text{MPa}) \quad (5.7)$$

If all the experimental results are compared with this model, the correspondence is still reasonably good, (see Fig.5.7). The standard deviation is found to be 0.061.

Finally, a model is obtained by combining the expressions (5.6) and (5.7):

$$v = k_2 \left( 0.8 - \frac{\sigma_c}{200} \right) \left( 1.0 - 1.2 \frac{e}{b} \right) \quad (5.8)$$

In the same way as for the model (5.6),  $k_2$  is determined to  $k_2 = 1.11$ . The results of this model are compared with the experimentally obtained  $v$  - values in Table 5.2. The coefficient of variation is calculated to 0.045, which is considerably less than for the expressions (5.6) and (5.7) alone.

The conclusion must then be that the empirical model which corresponds best with the experimental result of this report is

$$v = 1.11 \left( 0.8 - \frac{\sigma_c}{200} \right) \left( 1.0 - 1.2 \frac{e}{b} \right) \quad (5.9)$$

However, it should be emphasized that when results from test series from other laboratories (see Table 5.3) are included in the analysis, scatter is increased considerably. The coefficients of variation are approximately 0.07 - 0.08, and smallest for the model (1).

Thus, in this case, the model

$$v = 0.8 - \frac{\sigma_c}{200}$$

is concluded as producing the best correspondence with all available experimental results (see Fig. 5.8), i.e. it is therefore recommended to use this model for practical calculations.

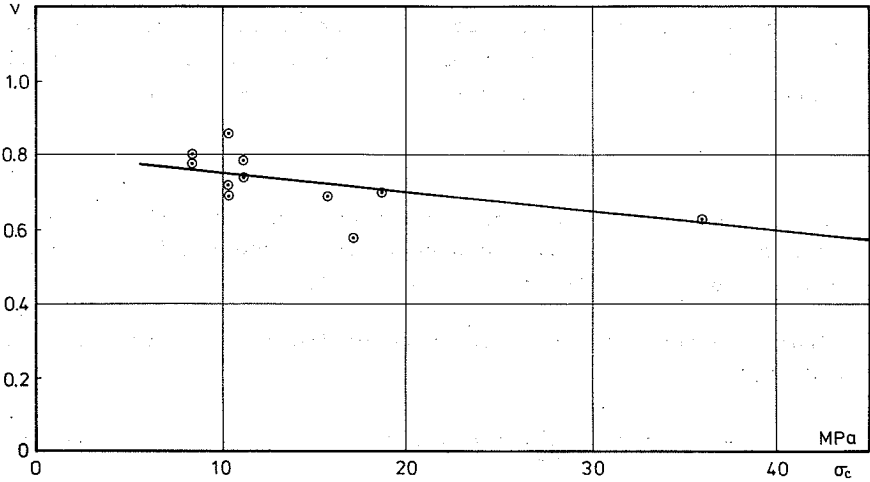


Fig. 5.7 The average  $\nu$  - values compared with the empirical expression  $\nu = 0.8 - \sigma_c/200$

Serie	$\nu$	$\bar{\nu}$
T	0.72	0.74
Tm	0.78	0.79
Td	0.72	0.69
V	0.59	0.63
U	0.68	0.70
Uc	0.56	0.58
Um	0.75	0.69
X	0.82	0.80
Xd	0.82	0.78
B	0.77	0.72
Bd	0.77	0.86

Table 5.2: Average  $\nu$ -values compared with the empirical expression

$$\nu = 1.11 (0.8 - \sigma_c/200) (1.0 - 1.2 e/b)$$

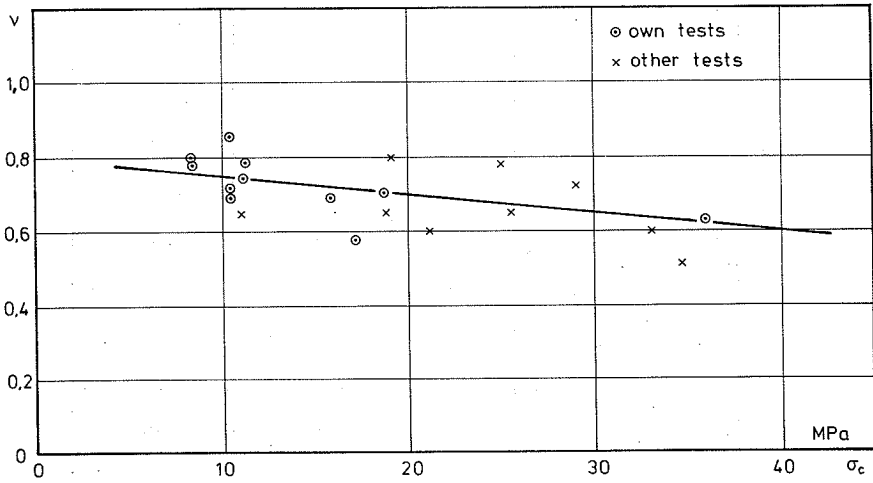


Fig. 5.8 The average  $\nu$  - values of own and other test series compared to the empirical model  $\nu = (0,8 - \sigma_c/200)$ .



Test series	Number of tests	Concrete strength $\sigma_c$ (MPa)	Effective-ness parameter ( $\bar{v}$ )
Malling [72.1]	13	10.5	0.65
Rathkjen [69.1]	7	25.0	0.78
Özden [67.3] H.C.Sørensen[71.1]	18	29.0	0.72
Placas [71.2] & Regan	15	33.0	0.60
Taylor [66.1]	3	21.1	0.60
Leonhardt and Walther[63.1]	10	19.1	0.80
Leonhardt and Walther [65.1]	4	18.8	0.65
Guralnick [59.1]	2	34.7	0.51
Hamadi [76.3]	5	25.5	0.65
Lyngberg [76.3]	9	30.0	0.76
Jensen [78.3] et al.	2	50.0	0.54

Table 5.3 Average  $\bar{v}$  - values of other test series.

## 6. FATIGUE TESTS

### 6.1 Purpose of Tests

The aim of the fatigue tests was not to produce a thorough investigation of the fatigue strength of beams in shear, but only to carry out a few pilot tests to get an indication of the fatigue strength of beams with shear reinforcement designed in accordance with the web crushing criterion.

### 6.2 Test Beams

The geometrical data of the test beams are given in Table 2.1, Fig. 2.2, and Fig.2.3. The concrete strength, yield force of stirrups and the average strength of the main reinforcement are given in Tables 3.2, 3.3, and 3.4, respectively. In Table 6.1, the reinforcement degree, the ultimate static shear load (calculated from (1.1a) with  $v = 0.7$ ), and the ultimate static flexural load (taken from table 2.1) are given.

Beam no	$P_y$ (kN)	$\sigma_c$ (MPa)	$\psi$ (%)	$V_u$ (kN)	$V_F$ (kN)	$V_{max}$ (kN)	$\frac{V_{max}}{V_u}$
U5604 p	11.00	24.1	4.35	244	328	120	0.49
U5606 p	13.60	18.5	7.01	233	328	116	0.50
U5606 q	14.05	20.6	6.50	251	328	190	0.76
U5606 r	13.40	16.4	7.78	216	328	160	0.74
U5606 s	13.90	20.2	6.10	247	328	153	0.62
U5610 p	10.45	17.4	12.50	280	328	137	0.49
T6007 p	13.80	13.5	4.87	144	290	80	0.56

Table 6.1 Results of fatigue tests

### 6.3 Testing of Beams

The loading diagram for the fatigue tests was identical with the diagram for the static tests, Fig.3.2.

In the actual test rig used for the fatigue tests, the movable support, built as a 3 m radius pendulum bearing for the static tests, was exchanged with a roller bearing. The reason for this was insufficient fatigue strength of the pendulum bars. The test rig is shown in Fig. 6.1.

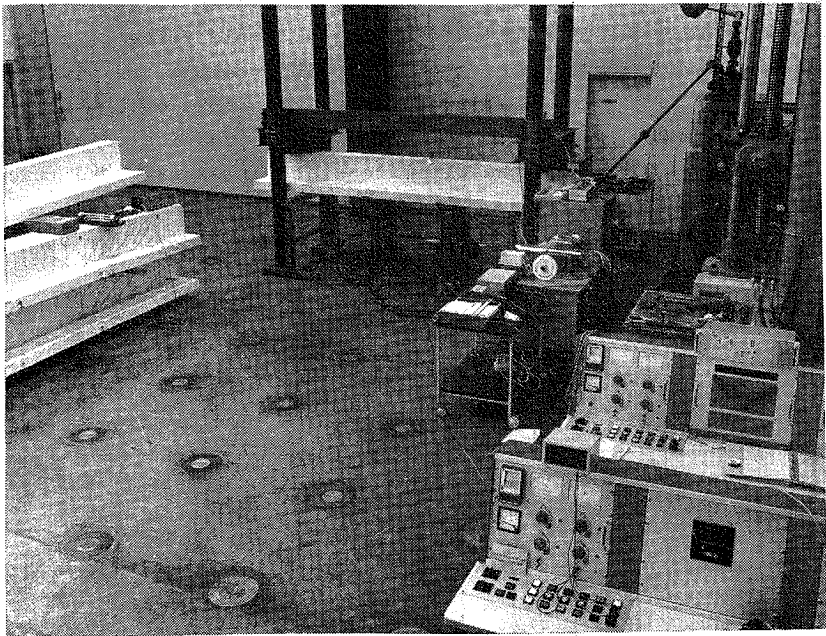


Fig.6.1 Test rig

The pulsation machine was an Amsler P960-SP1351. The frequency of the pulsation was 45 c/s and the form was sinusoidal with the minimum load equal to  $V_{\min} = 1.5 \text{ kN}$  and the maximum load equal to a certain fraction (in the interval 0.43-0.66) of the ultimate load (see Table 6.1 or 6.2).

The test was started as an ordinary static test. According to the procedure described in Section 3.5, the load was through several loading stages increased to  $V_{\max}$ . The stirrup stresses were recorded at each load stage. After unloading, the pulsation machine was started and the beam taken through a few hundreds of cycles whereupon the static test with registration of stirrup stresses was repeated.

## 6.4 Test Results

### 6.4.1 Fatigue Failures

The results of the tests are summarized in Table 6.2, where  $V_{\max}$ , the number of cycles before failure and the type of failure, are given. In Fig.6.2 - 6.7, the shear zones are shown after failure. Generally, it is seen that when the failure was fatigue failure of the stirrups, the failure section was always located in or near the stirrup bends.

Beam no	$V_{\max}$ (kN)	$\frac{V_{\max}}{V_u}$	Number of pulsations	Type of failure
U5604 p	120	0.49	$2.05 \cdot 10^6$	No failure
U5606 p	116	0.50	$8.65 \cdot 10^6$	Shear failure, stirrups
U5606 q	190	0.76	$0.02 \cdot 10^6$	Shear failure, concrete
U5606 r	160	0.74	$0.18 \cdot 10^6$	Shear failure, concrete
U5606 s	153	0.62	$0.17 \cdot 10^6$	Shear failure, stirrups
U5610 p	137	0.49	$1.27 \cdot 10^6$	Flexural failure, reinf.
T6007 p	80	0.56	$2.00 \cdot 10^6$	Shear failure, stirrups

Table 6.2 Results of fatigue tests



Fig.6.2: Fatigue failure of stirrups.  $V_{\max} = 0.5 V_u$



Fig.6.3: Fatigue failure of concrete struts.  $V_{\max} = 0.76 V_u$



Fig.6.4: Fatigue failure of concrete struts.  $V_{\max} = 0.74 V_u$



Fig.6.5: Fatigue failure of stirrups.  $V_{\max} = 0.62 V_u$

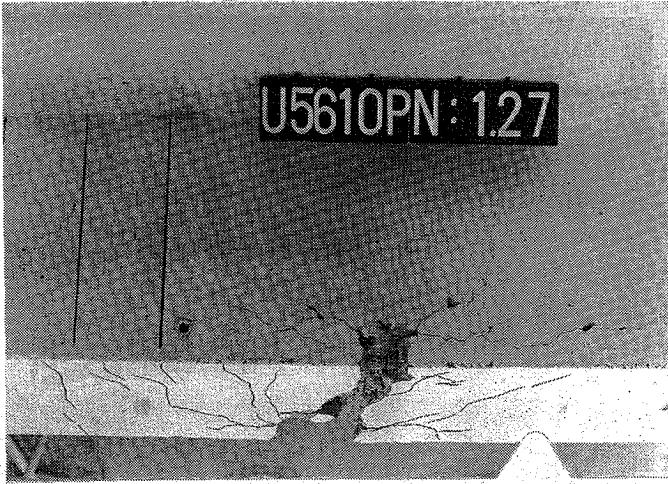


Fig.6.6: Fatigue failure of main reinforcing bars.

$$V_{\max} = 0.69 V_u$$

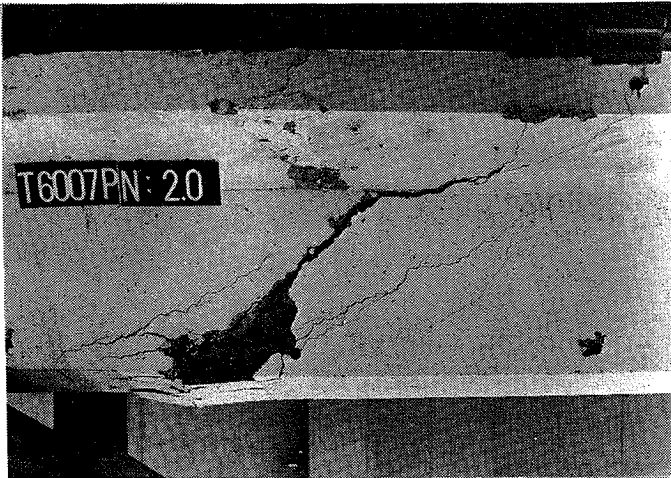


Fig.6.7: Fatigue failure of stirrups.  $V_{\max} = 0.56 V_u$

In Fig.6.8, the development of the cracks during the fatigue test of beam No. U5610p is demonstrated. It is seen from the penultimate picture that at this stage ( $1.13 \cdot 10^6$  pulsations), at least one of the main reinforcement bars has failed. The point of failure can be located as the point where the inclined anchorage cracks at the main reinforcement change direction.

After  $2.05 \cdot 10^6$  pulsations without obtaining the fatigue failure, the test of beam No.u5604p was stopped and the beam moved to the static test rig. The results of the static test (see Table 4.4) were failure loads of 235 kN and 225 kN for the shear spans E and W, respectively. This result indicates that the ultimate shear load calculated to 244 kN (see Table 6.1) is not influenced by the pulsations if these are stopped before fatigue failure is obtained.

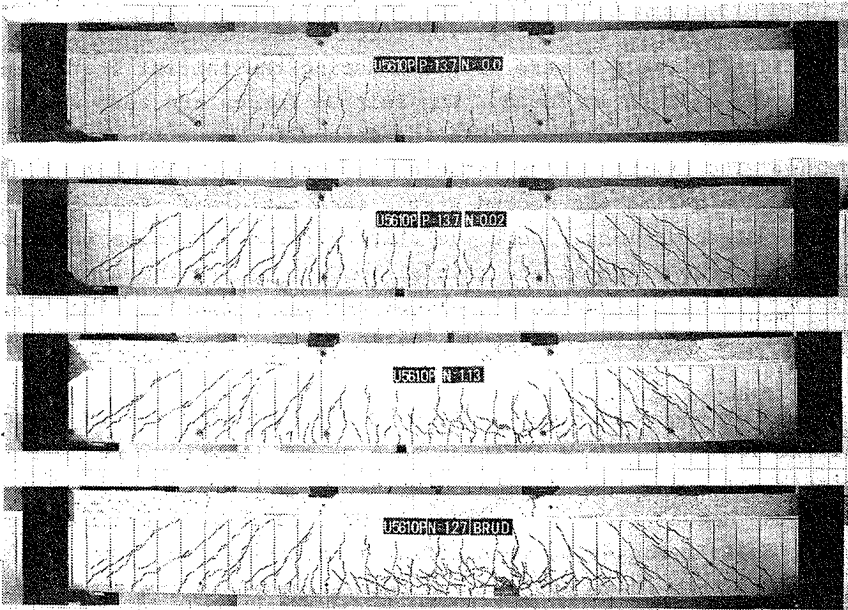


Fig.6.8 Development of the cracks during the fatigue test of beam No.U5610p (the maximum load in 137 kN (= 13.7 Mp). N is the number of pulsation in  $10^6$ )



Finally, it should be noted that the results of the fatigue test with beam No.U5606g is doubtful. In connection with a stop in the pulsations after 16700 cycles, the beam was mistakenly given a static load of between 80% and 100% of the ultimate load. This may be the reason for the premature fatigue failure. This suspicion is substantiated by the result of beam No.U5606 r. This test was very nearly a duplicate of the test of beam No.U5606g, but the number of pulsations before failure was about ten times bigger.

#### 6.4.2 Results of Stirrup Force Measurements

A typical result of the stirrup force measurements is shown in Fig. 6.9. Because of some experimental difficulties in bringing the load below  $V_{\min}$ , the zero-measurement of the stirrup strains was taken at  $V = V_{\min}$ . The stirrup force measurements shown with the full line in Fig.6.9 were produced during the initial static test. The usual picture is found. The stirrup forces are zero until the cracking load is reached, then the forces increase to the maximum value. The stirrup force measurements shown with the dotted lines were taken during the second static test performed after a small amount of pulsations. Here the stirrup forces increase instantly from the zero value at the initial load  $V_{\min}$  to the maximum value at  $V_{\max}$  and the curves are almost perfectly linear. The reason for this is that in the second static test, the cracks are established.

In each of the measurements given in Fig.6.10, the stirrup force at the load  $V_{\min}$  are taken as zero value. However, it is impossible for a crack to close completely upon unloading. This means that the actual stirrup force will never reach zero again after cracking. In Fig.6.10, this effect is demonstrated. The load is increased from 0 to 100 kN and then unloaded in the same load steps until zero. It is seen that a force of about 1.50 - 2.00 kN remains in the stirrups.

In Table 6.3, the recorded stirrup stresses at  $V_{\max}$  are given.

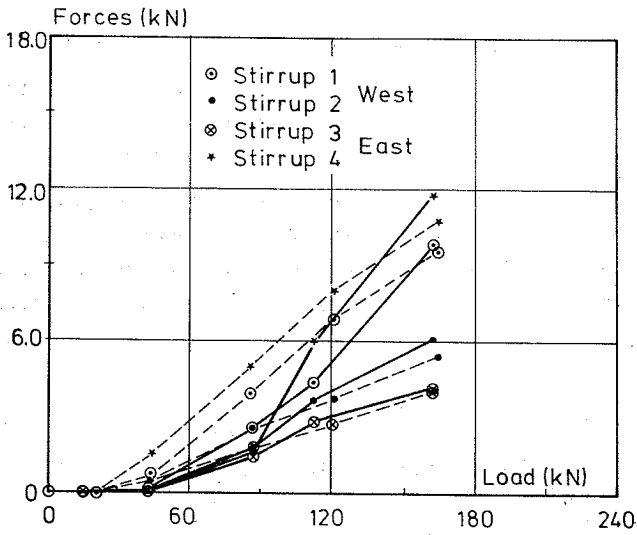


Fig.6.9 Stirrup force measurements

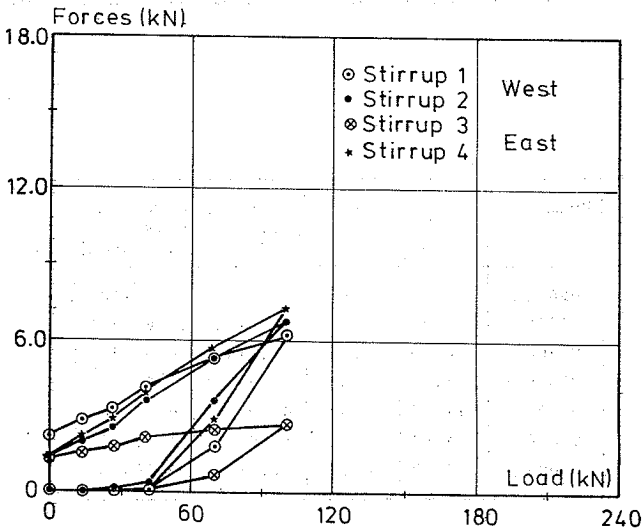


Fig.6.10 Stirrup force measurements

6.5 Discussion and Conclusions

The registered failures were caused by fatigue failure of the stirrups, fatigue failure of the concrete in the compression struts or fatigue failure of the main reinforcing bars.

The stirrup steel was mild steel. According to [75.2], there is the following relationship between the number of pulsations  $n$  before failure and the ratio between the stress in the stirrups at the maximum load  $\sigma_{u+}$  and the yield stress of the stirrup steel  $\sigma_y$ .

$$\frac{\sigma_{u+}}{\sigma_y} = \begin{cases} 1 & n < 10^5 \\ 2.25 - 0.25 \log n & 10^5 > n > 10^7 \\ 0.68 & n > 2 \cdot 10^6 \end{cases} \quad (6.1)$$

If  $\sigma_{u+}$  is taken to be equal to the stirrup stress at  $V_{max}$  recorded in Table 6.3,  $n$  can be calculated from (6.1). The results are given in Table 6.3, where the actual registered number of pulsations before failure are recorded for each beam for comparison.

Beam no.	$P_a$ kN	$\frac{P_a}{P_y}$	Number of pulsation (calcul.)	Number of pulsation (measured)
U5604 p	-	-	-	$2.05 \cdot 10^6$
U5606 p	6.80	0.50	$> 2.0 \cdot 10^6$	$8.65 \cdot 10^6$
U5606 q	14.05	1.00	$0.1 \cdot 10^6$	$0.02 \cdot 10^6$
U5606 r	11.80	0.88	$0.3 \cdot 10^6$	$0.18 \cdot 10^6$
U5606 s	12.95	0.93	$0.19 \cdot 10^6$	$0.17 \cdot 10^6$
U5610 p	4.41	0.42	$> 2.0 \cdot 10^6$	$1.27 \cdot 10^6$
T6007 p	9.27	0.67	$2.0 \cdot 10^6$	$2.00 \cdot 10^6$

Table 6.3 Stirrups stresses at  $V_{max}$  and measured and calculated number of pulsations

It is seen that for the beams where stirrup failure is registered, i.e. beams Nos. U5606p, U5606s, and T6007p the agreement between the calculated and the actual number of pulsation is very close.

The beams U5606q, U5606r, and U5610p failed at a number of pulsation considerably lower than predicted by equation ( 6.1). However, this is quite natural when it is noticed that U5606q and U5606r failed by fatigue failure of the concrete struts, and U5610p by fatigue failure of the main reinforcement. An estimate of the maximum stress in the concrete struts and the main reinforcement, respectively, shows that failure at a considerably lower number of  $n$  than calculated according to equation ( 6.1 ) could be expected.

In Fig.6.11, the Wöhler-diagramme for all fatigue tests are shown. Because of the mixture of different kinds of failures, the picture is rather unclear.

However, one main result can be stated: In all cases where  $V_{max}$  did not exceed  $0.56 V_u$ , the beam supported at least  $2 \cdot 10^6$  pulsations without failure.

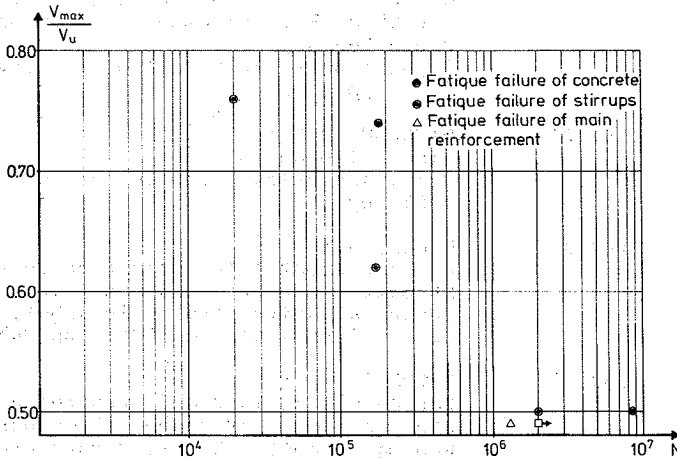


Fig.6.11 Wöhler-diagramme

REFERENCES

- [59.1] GURALNICK, S.A.:  
Shear Strength of Reinforced Concrete Beams.  
Journal of the Structural Division. Pro-  
ceedings ASCE Vol. 85, No. ST 1, 1959,  
pp 1-42.
- [63.1] LEONHARDT, F. & WALTHER, R.:  
Schubversuche an einfeldrigen Stahlbeton-  
balken mit und ohne Schubbewehrung.  
Deutscher Ausschuss für Stahlbeton.  
Heft 151, 1962, pp 83.
- [65.1] LEONHARDT, F. & WALTHER, R.:  
Geschweisste Bewehrungsmatten als Bügelbe-  
wehrung. Schubversuche an Plattenbalken  
und Verankerungsversuche.  
Die Bautechnik, Vol. 42, No. 10, 1965,  
pp 329-341.
- [66.1] TAYLOR, R.:  
Some Shear Tests on Reinforced Concrete  
Beams with Stirrups.  
Magazine of Concrete Research, Vol. 18, No.57,  
1966, pp 221-230.
- [67.1] NIELSEN, M.P.:  
Om forskydningsarmering i jernbetonbjælker.  
(On Shear Reinforcement in Reinforced Con-  
crete Beams).  
Bygningsstatistiske Meddelelser, Vol. 38, No. 2,  
1967, pp 33-58.
- [67.2] NIELSEN, M.P.:  
Discussion on [67.1].  
Bygningsstatistiske meddelelser, Vol. 40, No. 1,  
1969, pp 55-63.
- [67.3] ÖZDEN, K.:  
An Experimental Investigation on the Shear  
Strength of Reinforced Concrete Beams.  
Technical University of Istanbul, Faculty  
of Civil Engineering. 1967, pp 243.
- [69.1] RATHKJEN, A.:  
Forsøg med bjælker med afkortet armering.  
Danmarks Ingeniørakademi, Bygningsafdelingen.  
Ren og anvendt Mekanik. Report 6901, 1969,  
pp 14.

- [71.1] SØRENSEN, H.C.:  
Forskydningsforsøg med 12 jernbetonbjælker med T-tværsnit, Copenhagen Technical University of Denmark. Structural Research Laboratory. Report R20. 1971, pp 49.  
(English translation: Shear Tests on 12 Reinforced Concrete Beams. Report R60, 1974, pp 49).
- [71.2] PLACAS, A. & REGAN, P.E.:  
Shear Failure of Reinforced Concrete Beams. Journal of the ACI. Proc. Vol. 68, No.10 Oct. 1971, pp 763-773.
- [72.1] MALLING, V.:  
Forskydningsforsøg med jernbetonbjælker med kraftig bøjlearmering. Aalborg. Danmarks Ingeniørakademi. Bygningsafdelingen. Ren og Anvendt Mekanik. Report 7202, 1972, pp 9.
- [74.1] JENSEN, B.C.:  
Koncentrerede belastninger på uarmerede betonprismer. (Concentrated Loads on Plain Concrete Prisms). Bygningsstatistiske Meddelelser. Vol. 44, No. 4, December 1974, pp 89-111.
- [75.1] NIELSEN, M.P., & BRÉSTRUP, M.W.:  
Plastic Shear Strength of Reinforced Concrete Beams. Bygningsstatistiske Meddelelser. Vol. 46, No. 3, 1975, pp 61-99.
- [75.2] NIELSEN, M.P.:  
Beton 1, Del 1, 2 og 3. Aalborg/København 1975, pp.678.
- [76.1] BRÉSTRUP, M.W., NIELSEN, M.P., BACH, F. & JENSEN, B.C.:  
Shear Test on Reinforced Concrete T-beams. Series T. Copenhagen. Technical University of Denmark. Structural Research Laboratory. Report No.R75, 1976, pp.114.
- [76.2] HAMADI, Y.D.:  
Force Transfer Across Cracks in Concrete Structures. London, The Polytechnic of Central London. School of the Environments. Ph.D: Thesis. May 1976, pp.503 + App.

- [76.3] LYNGBERG, B.S.:  
Ultimate Shear Resistance of Partially Pre-  
stressed Reinforced Concrete I-Beams.  
ACI-Journal, April 1976, No.4, pp.214-222.
- [77.1] BRÆSTRUP, M.W., NIELSEN, M.P. & BACH, F.:  
Plastic Analysis of Shear in Concrete.  
Zeitschrift für Angewandte Mathematik und  
Physik, Vol.58, 1978, pp.3-14.
- [78.1] NIELSEN, M.P., BRÆSTRUP, M.W., & BACH, F.:  
Rational Analysis of Shear in Reinforced  
Concrete Beams.  
International Association for Bridge and  
Structural Engineering. Proceedings P-15/78.  
May 1978, pp 16.
- [78.2] NIELSEN, M.P., BRÆSTRUP, M.W., JENSEN, B.C. &  
BACH, F.:  
Concrete Plasticity. Beam Shear-Punching  
Shear-Shear in Joints.  
Copenhagen. Danish Society for Structural  
Science and Engineering. Special publi-  
cation, October 1978.
- [78.3] JENSEN, J.F., PEDERSEN, C., BRÆSTRUP, M.W.,  
BACH, F., & NIELSEN, M.P.:  
Rapport over forskydningsforsøg med 6  
spændbetonbjælker.

AFDELINGEN FOR BÆRENDE KONSTRUKTIONER

DANMARKS TEKNISKE HØJSKOLE

Structural Research Laboratory

Technical University of Denmark, DK-2800 Lyngby

RAPPORTER (Reports)

(1977 - )

- R 81. Resumeoversigt 1976. Summaries of papers 1976. 1977.
- R 82. MØLLMANN, H.: Static and dynamic analysis of plane cable structures. 1977.
- R 83. RIBERHOLT, H.: Bolte indlimet i limtræ. 1977.
- R 84. AGERSKOV, H. and J. BJØRNBAK-HANSEN: Fatigue strength of welded connections in round bar steel structures. 1977.
- R 85. LAURSEN, M.E., M.P. NIELSEN and M. ROIKJØR: Stability analysis of beams and arches by energy methods. 1977.
- R 86. LAURSEN, M.E.: Derivation of symmetric integration formulas for triangles. 1977.
- R 87. LAURSEN, M.E.: Stability and vibration analysis of plane curved beams by an equilibrium finite element method. 1977.
- R 88. PEDERSEN, FLEMMING BLIGAARD: Vibration analysis of viscoelastically damped sandwich structures. 1978.
- R 89. BRØNDUM-NIELSEN, TROELS: Epoxy resin repair of cracked concrete beams. 1978. \*)
- R 90. HESS, UWE, B.CHR. JENSEN, M.W. BRÆSTRUP, M.P. NIELSEN og FINN BACH: Gennemlokning af jernbetonplader. 1978.
- R 91. HANSEN, KARL ERIK, KAJ L. BRYDER og M.P. NIELSEN: Armeringsbestemmelse i jernbetonskaller. 1978.
- R 92. ASKEGAARD, V.: Stress and strain measurements in solid materials. 1978.
- R 93. SCHMIDT, HENRIK: Udbredelse af akustisk emission i beton. 1978.
- R 94. BYSKOV, ESBEN og STEEN KRENK: Konstruktionstræs mekaniske styrke. 1978.
- R 95. Resumeoversigt 1977. Summaries of papers 1977. 1978.
- R 96. DYRBYE, CLÆS: Admittance-curves. ZILSTORFF, ANNE and CLÆS DYRBYE: Admittance of bars. 1978.
- R 97. DYRBYE, CLÆS: Dynamic systems with sinusoidal mode shapes. 1978.
- R 98. ANDRESEN, CLÆS: Bjælker og søjler med åbne, tyndvægede tværsnit. 1978.
- R 99. RIBERHOLT, H.: Eingeleimte Gewindestangen. 1978.
- R 100. PEDERSEN, C.: Opbøjet længdearmering som forskydningsarmering. 1978.
- R 101. JENSEN, J.F., M.W. BRÆSTRUP, F. BACH og M.P. NIELSEN: Nogle plasticitetsteoretiske bjælkeløsninger. 1978.
- R 102. JENSEN, J.F., C. PEDERSEN, M.W. BRÆSTRUP, F. BACH og M.P. NIELSEN: Rapport over forskydningsforsøg med 6 spændbetonbjælker. 1978.
- R 103. JENSEN, J.F., V. JENSEN, H.H. CHRISTENSEN, F. BACH, M.W. BRÆSTRUP and M.P. NIELSEN: On the behaviour of cracked reinforced concrete beams in the elastic range. 1978.

\*) Udsolgt. Out of print.



- R 104. ANDERSEN, ERIK YDING: Konstruktionsovervågning med akustisk emission. Prøvebelastning af landevejsbro. 1979.
- R 105. FREDSCGAARD, SØREN SKYTTE: Ligevægts-elementer i de finite elementers metode. Formulering og beregningsgang. 1979.
- R 106. AGERSKOV, HENNING: Tests on high-strength bolted T-stub connections. 1979.
- R 107. KIRK, JENS: Direkte beregning af imperfekte skalkonstruktioner. 1979.
- R 108. Resumeoversigt 1978. Summaries of papers 1978. 1979.
- R 109. BRØNDUM-NIELSEN, TROELS: Stress analysis of concrete sections under service load. 1979.
- R 110. BRÆSTRUP, M.W.: Effect of main steel strength on the shear capacity of reinforced concrete beams with stirrups. 1979.
- R 111. BRINCKER, RUNE: Murede vægges tværbæreevne. En undersøgelse af murværks fysiske egenskaber. 1979.
- R 112. GIMSING, NIELS J.: Analytisk undersøgelse af materialforbruget for plane kabelsystemer med ensformig fordelt belastning. 1979.
- R 113. MADSEN, HENRIK OVERGAARD: Load models and load combinations. 1979.
- R 114. RIBERHOLT, H. and P. HAUGE MADSEN: Strength distribution of timber structures. Measured variation of the cross sectional strength of structural lumber. 1979.
- R 115. PEDERSEN, MAX ELGAARD: En generel beregningsmetode for betontværsnit. 1980.
- R 116. PEDERSEN, MAX ELGAARD: Kipstabilitet af armerede betonbjælker. 1980.
- R 117. BRYDER, KAJ L.: Optimeringsmetoder for 2-dimensionale legemer af ideal-plastisk materiale. 1980.
- R 118. DUKOW, EWTIM N.: Optimale Projektierung von vorgespannten Brückenträgern. 1980.
- R 119. PEDERSEN, HENNING: Optimering af jernbetonplader. 1980.
- R 120. BACH, FINN, M.P. NIELSEN and M.W. BRÆSTRUP: Shear tests on reinforced concrete T-beams. Series V, U, X, B and S. 1980.